NASA CR-111892

THE INFLUENCE OF SPACE RADIATION UPON THE MOS MICROMETEOROID CAPACITOR DETECTOR

By

L. K. Monteith

R. P. Donovan

M. Simons

Prepared for

National Aeronautics and Space Administration
Langley Research Center
Langley Station
Hampton, Virginia

Final Report

February 1971

(Prepared under Contract NAS1-10232 by the Engineering and Environmental Sciences Division of the Research Triangle Institute, Research Triangle Park, North Carolina.)

CONTENTS

LIST OF ILLUSTRATIONS

FOREWORD

This study was sponsored by the Meteoroid Section of the Space Technology Division, NASA Langley Research Center, Hampton, Virginia. J. Siviter was the NASA Technical Monitor. The contract period extended from July 17, 1970 to February 16, 1971.

SECTION I

INTRODUCTION AND SUMMARY

The purpose of this study is to assess the magnitude of the influence of space radiation upon the MOS capacitor detectors to be flown on MTS. These capacitor detectors are metal-oxide silicon (MOS) structures of a large area (~ 20 cm^2) fabricated by the thermal oxidation of silicon to form an oxide either 0.4 μm thick or 1.0 μm thick. To complete this structure an aluminum electrode 0.1 μm thick is evaporated on top of the oxide. The oxide is stripped from the bottom side of the wafer and a second aluminum evaporation makes contact to this side of the capacitor. The doping of the silicon is high so as to minimize changes in the capacitance with voltage. The operation of the capacitor as a micrometeoroid detector depends upon the triggering of a capacitor discharge by micrometeoroid impact followed by a self-healing interaction.

The counting circuit of the satellite responds to capacitor discharge pulses greater than 6 volts. The bias applied to the capacitors varies with oxide thickness, the 0.4 μm oxide capacitor being biased at +40 volts on the aluminum and the 1.0 μm oxide thick capacitor, 60 volts. Each capacitor has a 1 MΩ resistor in series with it so that the power drain through a defective capacitor is limited even in the event of a short circuit.

Four possible failure modes are considered in this study: 1) spurious output generated by photocurrents; 2) spurious output due to accumulation of space charge in the oxide; 3) spurious output because of spontaneous discharge of space charge in the oxide; and 4) detector failure because of increased capacitor leakage (dark) current.

The first two possibilities are discussed in sections II and III, respectively, and are dismissed as negligible. The significance of the last two is less certain.

The analysis in section IV concludes that a spontaneous discharge, if it occurs, is not likely to create a signal of sufficient magnitude to trigger the counting circuit if only the space charge within the oxide participates in the spontaneous discharge. This conclusion assumes that the spontaneous discharge occurs over only a small fraction of the total volume of the space charge and that only a small fraction of the total space charge participates in spontaneous discharge. Complete discharge of the radiation-induced charge buildup, which is distributed over the capacitor area, is unlikely to occur through a small localized

region initiated by a spontaneous discharge. The more probable failure mechanism is for the spontaneous discharge to initiate a capacitor discharge, which would be indistinguishable from a capacitor discharge triggered by a micrometeoroid count and an error most certainly would result. No information exists on which to assess the likelihood of this event. The problem is best handled experimentally.

The MOS Detector Capacitors can also be rendered inoperative by greatly increased leakage current because of radiation-induced degradation of the oxide or the oxide-silicon interface. Conceptual models for assessing the importance of this problem are also inadequate, primarily because the leakage current of the capacitor is determined by defects rather than the properties of the intrinsic oxide. The influence of high-energy radiation upon these defects is completely speculative, but can be easily determined experimentally.

Two experiments are recommended to assure the reliability and accuracy of the MOS Detector output:

1) Irradiation of a biased detector with 20 keV electrons in order to maximize space charge buildup and the likelihood of a count being triggered by spontaneous discharge of the oxide space charge which in turn initiates a capacitor discharge.

2) Irradiation of a biased detector with 300 keV electrons to induce displacement damage and assess the likelihood of failure attributable to increased leakage currrent through the capacitor.

These radiation tests are simple and inexpensive to perform. They can easily simulate worse cases and, if no failure or spurious counts result, the influence of Van Allen belt irradiation upon the MOS Detector can be assumed negligible with high confidence. If failures or false counts are encountered, more realistic simulation is required before a realistic radiation-related limit is established.

The only type of radiation considered throughout this study is electrons of various energies; the influence of other types of space radiation have been assumed to be similar. No distinction has been made between the influence of electrons, protons, gamma rays or other high-energy radiation. This assumption is based on the radiation forecast to be encountered during the MTS mission.

SECTION II

ELECTRON-BOMBARDMENT-INDUCED-CONDUCTIVITY (EBIC)

Electron-bombardment-induced conductivity (EBIC) is a consequence of electron-hole pair production. Bombarding electrons transfer energy to a solid through the mechanism of electron-electron interactions, resulting in internal ionization. The ionized electrons have finite lifetime and mobility. Under the influence of an electric field they drift away from their ionization sites. This drift constitutes a current flow which adds to the drift of thermally ionized electrons. If the ionization sites are mobile, they also contribute a current component called hole current.

EBIC depends upon: (1) the energy loss mechanisms associated with the bombarding electrons, and (2) the drift of ionized electrons (and holes) in an applied electric field.

Energy Loss Mechanisms. - To describe the energy loss of a high energy bombarding electron beam we start with the Thomas-Whiddington (refs. 2.1, 2.2] relationship,

$$E_p^2 - E_p^2(x) = b\rho x \qquad (2\text{-}1)$$

where E_p is the energy of the bombarding electrons,

$E_p(x)$ is the electron energy at a depth, x, within the solid,

b is a material parameter and

ρ is the material density.

Figure 1 illustrates the geometry. Assuming that all the electron energy is given up in a distance less than L, we may define a range, R, by $E_p(R) = 0$ in eq. 2-1 so that

$$E_p^2 = b\rho R \; . \qquad (2\text{-}2)$$

R is the mean path length of the bombarding electrons in the solid. This result is consistent with the range-energy relationship for monoenergetic electrons given by Evans [ref. 2.3]. From eqs. 2-1 and 2-2 the rate of energy loss is

$$\frac{dE_p(x)}{dx} = -\frac{E_p}{2R\sqrt{1 - x/R}} \; . \qquad (2\text{-}3)$$

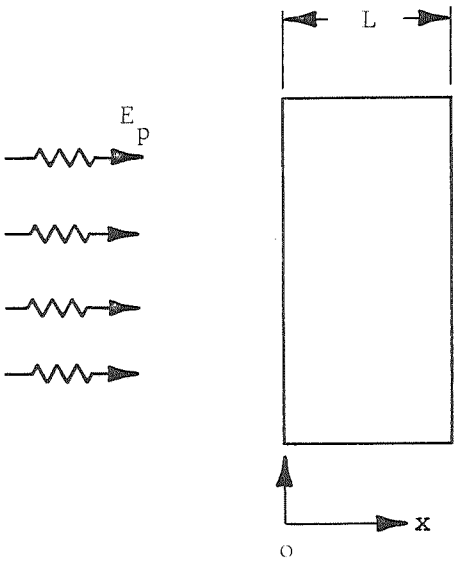

Figure 2.1. Geometry for EBIC Analysis

If we normalize the energy and distance to $\frac{E_p(x)}{E_p}$ and $\frac{x}{R}$, we obtain

$$\frac{d\left(\frac{E_p(x)}{E_p}\right)}{dx} = -\frac{1}{2R\sqrt{1 - x/R}} \qquad (2\text{-}4)$$

where the negative sign indicates that the electron energy loss decreases with increasing x. Figure 2.2 is a plot of eq. 2-4 with the energy loss in units of -1/2R. The salient feature is the near constant energy loss over the first half of the electron range. This result is substantiated by Young for 10 keV electrons in 1 μm aluminum oxide films. Our interest will also focus on low energy electrons, because the thickness of silicon oxide in the MOS Detector is also on the order of one micron. The worst case analysis must include electron energies which are the most efficient with regards to EBIC.

To describe the bombarding electron beam intensity at x, we use Lenard's relationship [ref. 2.4]

$$\frac{dJ_p(x)}{dx} = -\alpha J_p(x) \qquad (2\text{-}5)$$

where $J_p(x)$ is the bombarding current density at x in the solid and α, an absorption coefficient which depends upon energy $E_p(x)$ according to

$$\alpha = \frac{\alpha_o}{E_p^2(x)} . \qquad (2\text{-}6)$$

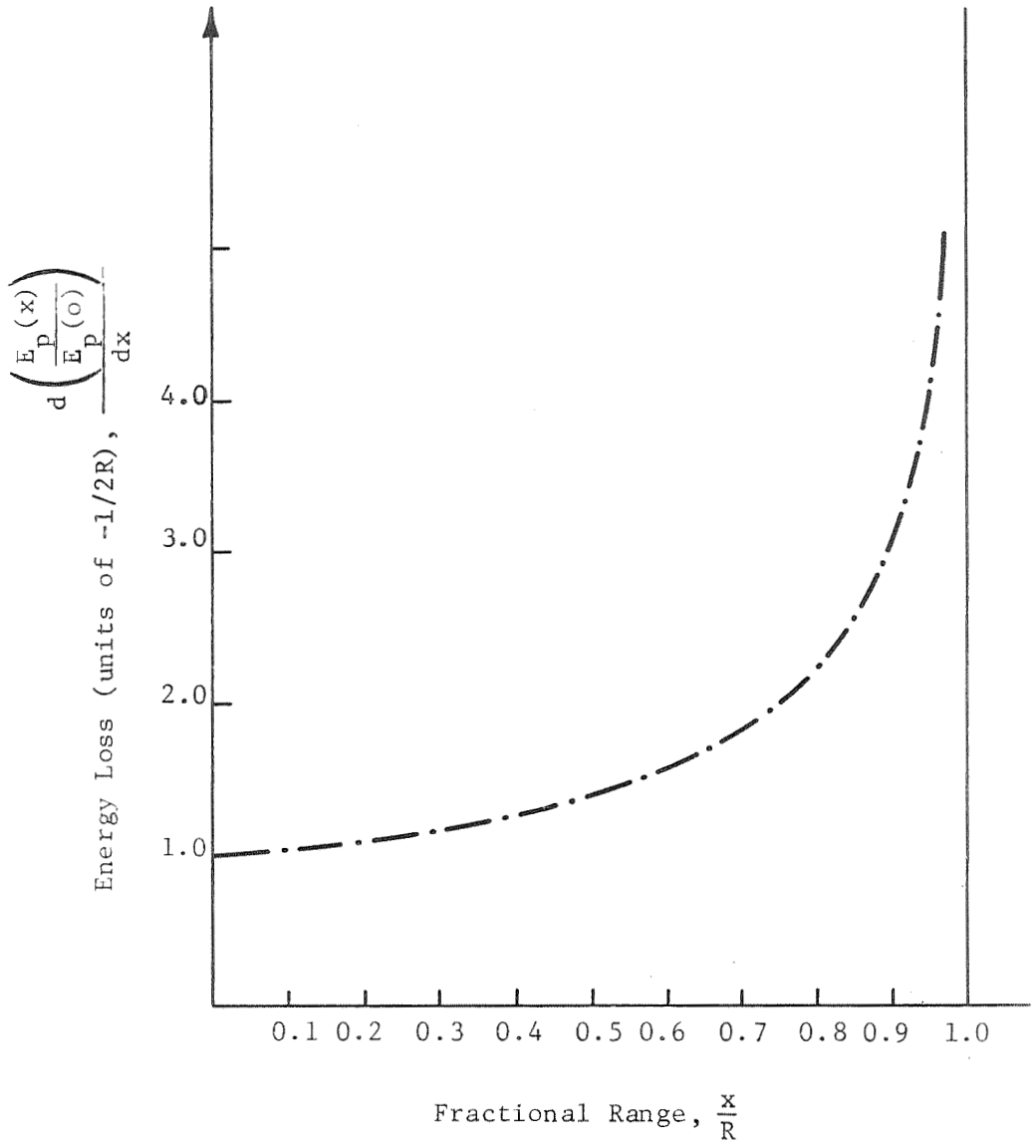

Figure 2.2. Energy Loss of Bombarding Electrons as a Function of Depth

Combining eqs. 2-1, 2-5 and 2-6,

$$\frac{dJ_p(x)}{dx} = - \frac{\alpha_o}{E_p^2 - b\rho x} J_p(x) \ . \qquad (2\text{-}7)$$

Upon integrating from o to x, or from $J_p(o)$ to $J_p(x)$ one obtains

$$J_p(x) = J_p(o)\left(1 - \frac{b\,x}{E_p^{\,2}}\right)^{\frac{\alpha_o}{b\rho}} . \qquad (2\text{-}8)$$

Since $E_p^{\,2} = b\rho R$,

$$\frac{J_p(x)}{J_p(o)} = \left(1 - \frac{x}{R}\right)^{\frac{\alpha_o}{b\rho}} . \qquad (2\text{-}9)$$

Eq. 2-9 gives the decrease in beam current as a function of depth of penetration.

Charge Transport in SiO_2. - For the analysis of EBIC we will assume the contacts to be ohmic. In Section IV, the contacts will be considered to be blocking, while in Section V injecting contacts will be considered. In each case the assumption regarding the electrical contacts is chosen to correspond to worst case analysis. In Section IV blocking contacts result in the build up of internal polarization as a result of electron bombardment while in Section V injecting contacts provide a mechanism through which dielectric loss or dissipation factor may depend upon irradiation.

To analyze the induced conductivity we consider the conduction electron density to be

$$n = n_e + n_o \qquad (2\text{-}10)$$

where n_e is the excess or electron bombardment induced contribution and n_o is the thermal contribution. Under the assumption of a simple lifetime process the excess electron density is governed by the rate equation

$$\frac{\partial n_e}{\partial t} = g_E . \qquad (2\text{-}11)$$

where g_E is the generation rate of excess electrons by the irradiation and τ is the electron lifetime. In steady state

$$n_e = g_E \tau_n . \qquad (2\text{-}12)$$

Under the assumption of ohmic contacts the electrical current density is given by

$$J = q\mu n E \tag{2-13}$$

where

q is the electronic charge,

μ is the conduction electron mobility,

n is the total carrier concentration, and

E is the applied electric field.

Combining eqs. 2-10, 2-12, 2-13,

$$J = q\mu(n_e + n_o)E = q\mu(g_E\tau_n + n_o)E \ . \tag{2-14}$$

Solving for E

$$E = \frac{J}{q\mu(g_E\tau_n + n_o)} = -\frac{dV_a}{dx} \tag{2-15}$$

assuming the geometry in Fig. 2.3. We have not restricted the spatial dependence of g_E or n_o. We could proceed in a general way; however, extensive computation can be avoided by some simplifying assumptions regarding the generation of excess electrons.

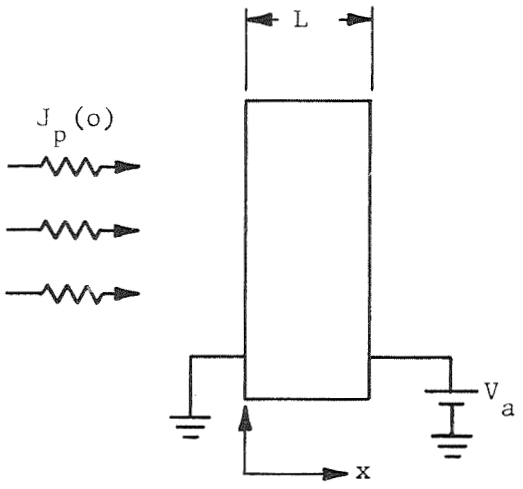

Figure 2.3. EBIC Geometry with Bias

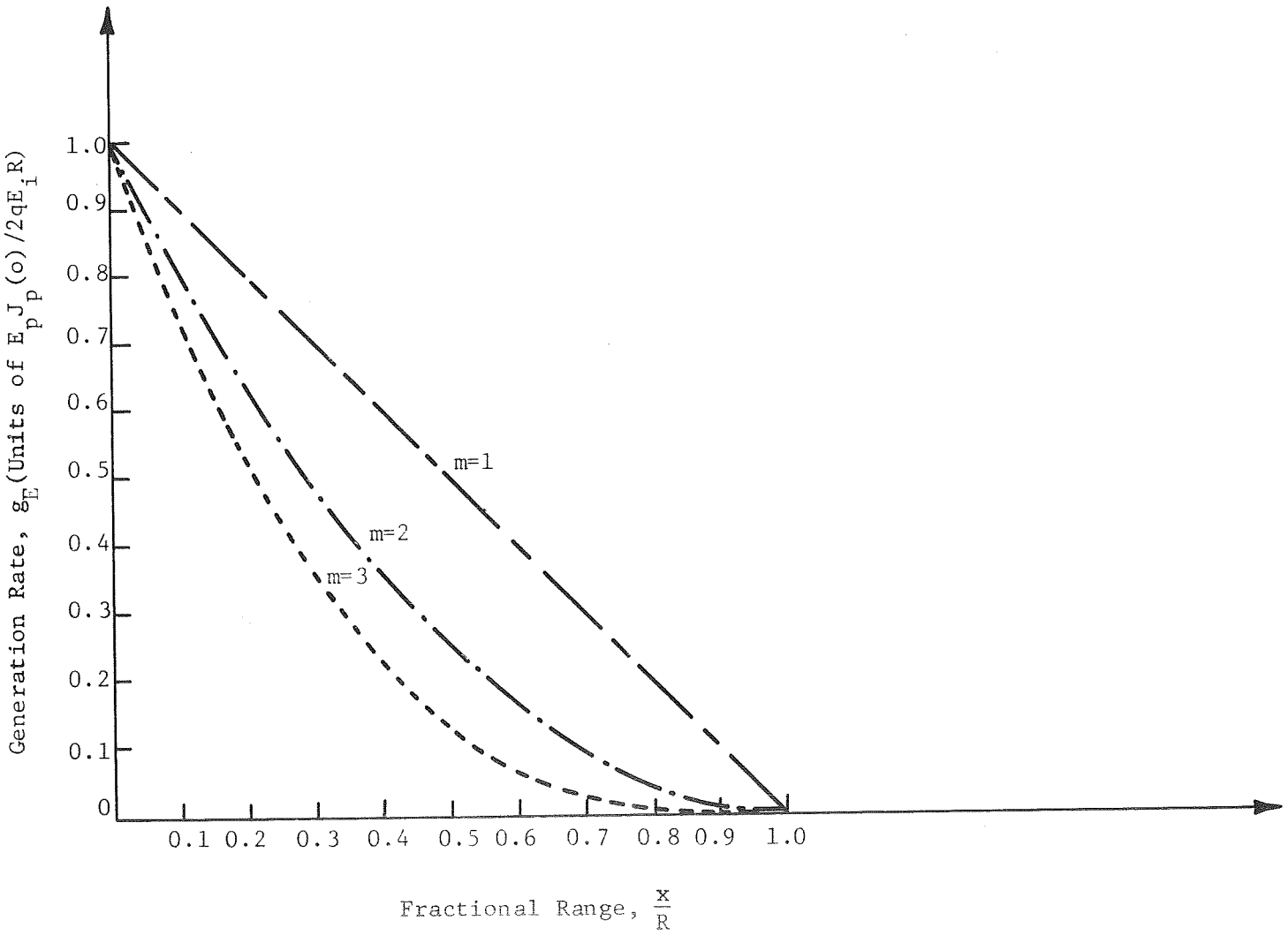

Figure 2.4. Calculated Electron Generation Rate as a Function of Depth

The generation of excess conduction electrons can be approximated by

$$g_E(x) = - \frac{dE_p(x)}{dx} \frac{J_p(x)}{q\ E_i} \qquad (2\text{-}16)$$

where the rate of energy loss is described by eq. 2-3 and the irradiation current density by eq. 2-9. The q in the denominator of eq. 2-16 converts current density to a particle density; E_i is the mean ionization energy for the excess conduction electrons. Introducing eqs. 2-3 and 2-9 into 2-16 yields,

$$g_E(x) = \left(\frac{E_p J_p(o)}{2qE_i R}\right)\left(1 - \frac{x}{R}\right)^m \qquad (2\text{-}17)$$

where $m = \frac{\alpha_o}{b\rho} - \frac{1}{2}$ and is greater than unity.

Experimental data by Pensak indicates that $1<m<3$ for SiO_2 [Ref. 2.5] and in Fig. 2.4, eq. 2-17 is plotted for the values of m = 1, 2, 3. The salient features are the well behaved nature of the results and the general trend for g_E to be appreciable only over a fraction of the range R for m = 3. To facilitate the analysis we choose to use an average constant value for g_E as opposed to the depth varying results of Fig. 2.4.

Using an average generation rate Fig. 2.5 represents the model for which we seek a solution. The excess electron concentration is given by

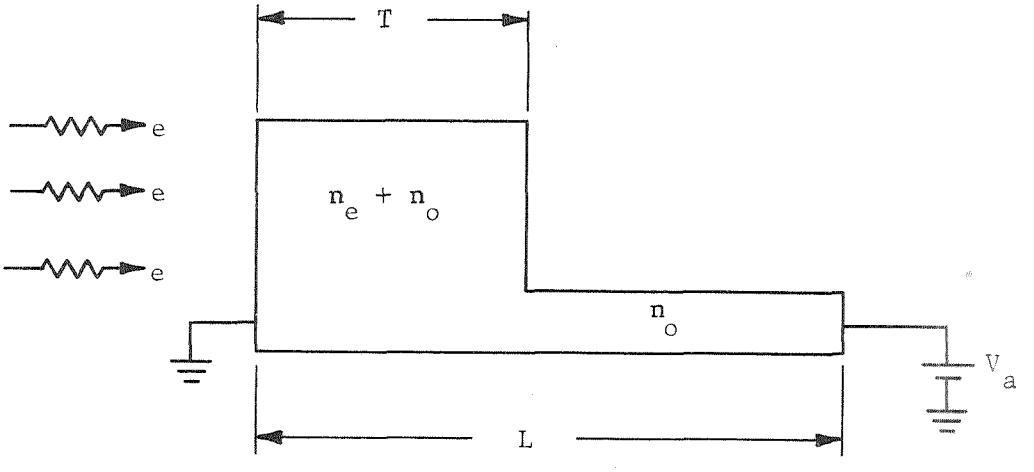

Figure 2.5. Simplified Generation Approximation

$$\frac{\partial n_e}{\partial t} = \bar{g}_E - \frac{n_e}{\tau_n} \tag{2-18}$$

where $\bar{g}_E$ is a constant from x = 0 to x = T and T is determined by the condition that $g_E(T)\ \tau_n \approx n_o$. At the distance T the spatially dependent excess carrier concentration is equal to the thermally excited carrier concentration. In steady state

$$n_e = \bar{g}_E \tau_n \tag{2-19}$$

and

$$E = \frac{J}{q\mu(\bar{g}_E \tau_n + n_o)} = -\frac{dV}{dx} . \tag{2-20}$$

Assuming J is constant through $0 \leq x \leq L$ eq. 2-20 can be integrated

$$\int_o^{V_a} dV = -\frac{J}{q\mu}\left\{\int_o^T \frac{dx}{\bar{g}_E \tau_n + n_o} + \int_T^L \frac{dx}{n_o}\right\} \tag{2-21}$$

to yield the current density J,

$$J = -\frac{q\mu_n V_a \bar{g}_E \tau_n n_o}{\bar{g}_E \tau_n (L-T) + n_o T} \tag{2-22}$$

assuming $g_E \tau_n >> n_o$ between o and T. Since the unirradiated current, J_o, is

$$J_o = q\mu_n n_o \frac{V_a}{L} \tag{2-23}$$

we may define the ratio of the current density of the irradiated solid, J, to the incident electron beam current density, $J_p(o)$, as

$$z = \frac{J}{J_p(o)} = -\frac{J_o}{J_p(o)}\left[\frac{1}{1 - \frac{T}{L}\left(1 - \frac{n_o}{\bar{g}_E \tau_n}\right)}\right] . \tag{2-24}$$

Finally defining $z_o = - J_o/J_p(o)$ yields

$$\frac{z}{z_o} = \frac{1}{1 - \frac{T}{L}\left(1 - \frac{n_o}{\bar{g}_E \tau_n}\right)} \tag{2-25}$$

We should consider eq. 2-25 in three parts. As before, the worst case analysis includes the assumption that $\bar{g}_E \tau_n >> n_o$. With this assumption, the first range we will consider is T <<L. Then

$$\frac{z}{z_o} \cong 1, \; T << L. \tag{2-26}$$

As T approaches L and with

$$\left(1 - \frac{T}{L}\right) > \frac{n_o}{\bar{g}_E \tau_n} \tag{2-27}$$

we obtain

$$\frac{z}{z_o} \cong \frac{1}{1 - \frac{T}{L}}, \; T \lesssim L . \tag{2-28}$$

When T = L, the solution is

$$\frac{z}{z_o} = \frac{\bar{g}_E \tau_n}{n_o}, \; T = L . \tag{2-29}$$

To proceed we must obtain an expression for the ratio $\frac{T}{L}$ and for $\bar{g}_E$. An expression for T can be obtained from eqs 2-17 and 2-19:

$$g_E(T)\tau_n = n_o = \frac{b\rho J_p(o)\tau_n}{2qE_i E_p}\left(1 - \frac{b\rho T}{E_p^2}\right)^m . \tag{2-30}$$

Solving for T yields

$$T = \frac{E_p^2}{b\rho}\left[1 - \left(\frac{2\,J_o}{J_p(o)}\,\frac{E_i}{E_o}\,\frac{E_p}{E_o}\,\frac{\tau_L}{\tau_n}\right)^{1/m}\right] \tag{2-31}$$

where $\tau_L = \frac{L^2}{\mu_n V_a}$ is the transit time for the electron across the sample length and $E_o = \sqrt{Lb\rho}$ is the incident energy required to penetrate the film (R=L). The case where $E_i << E_o$ (or the mean ionization energy is much less than the penetration energy) and the other ratios are comparable is of primary importance. For this case,

$$T \simeq \frac{E_p^2}{b\rho} = R \tag{2-32}$$

where R is the range of the incident electron in the solid, or

$$\frac{T}{L} \simeq \frac{E_p^2}{E_o^2} . \tag{2-33}$$

Thus, from eq. 2-28,

$$\frac{z}{z_o} \simeq \frac{1}{1 - \left(\frac{E_p}{E_o}\right)^2} \qquad T \lesssim L . \tag{2-34}$$

The average generation rate for $0 \leq x \leq T$ is determined from eq. 2-17:

$$\overline{g}_E = \frac{\frac{E_p J_p(o)}{2qE_i R} \int_o^T \left(1 - \frac{x}{R}\right)^m dx}{\int_o^T dx} . \tag{2-35}$$

Replacing the integration limit T by R using the approximations which yields eq. 2-32 and introducing the change of variable $y = \frac{x}{R}$ in eq. 2-35 yields

$$\overline{g}_E = \frac{E_p J_p(o)}{2qE_i R} \int_o^1 (1-y)^m \, dy \tag{2-36}$$

or finally

$$\overline{g}_E = \frac{E_p J_p(o)}{2qE_i R(m+1)} . \tag{2-37}$$

For R = L introducing eq. 2-37 into eq. 2-29 yields

$$\frac{z}{z_o} = \frac{E_o J_p(o) \tau_n}{2qE_i R(m+1)n_o} , \quad R = L; \tag{2-38}$$

which, upon substituting J_o and τ_L, reduces to:

$$\frac{z}{z_o} = \frac{1}{2} \frac{\tau_n}{\tau_L} \frac{E_o}{E_i} \frac{J_p(o)}{J_o} \frac{1}{m+1} . \tag{2-39}$$

Shown in Fig. 2.6 are the results of eq. 2-26 and 2-34 (solid lines) and eq. 2-39 (broken lines). The salient feature is that EBIC is not important until the energy of the incident beam is approximately equal to the energy necessary to penetrate the solid (until $E_p \sim E_o$). The scale for z/z_o is broken with its value at $E_p = E_o$ determined by the ratio of electron lifetime to transit time and by the ratio of energy of the primary electron to the mean ionization energy. The major result is that there is not an extreme for $0 \leq E_p \leq E_o$. Thus, we must look for a maximum z with $E_p > E_o$.

Before calculating the maximum z we should briefly consider the use of an average generation rate. For our problem we will be interested in a geometry crudely approximated in Fig. 2.7. This approximates a penetrating beam where the generation rate is finite throughout $0 < x < L$ and the thickness of the sample L is half the range of the primary electron. From eq. 2-15 we should consider

$$\frac{J}{q\mu} \int_o^L \frac{dx}{g_E \tau_n + n_o} = - \int_o^{V_a} dV_a \tag{2-40}$$

If $g_E \tau_n >> n_o$ through $0 \leq x \leq L$

$$V_a \simeq - \frac{J}{q\mu\tau_n} \int_o^L \frac{dx}{g_E} . \tag{2-41}$$

From the geometry of Fig. 2.7,

$$g_E = 1 - \frac{x}{R} = 1 - \frac{x}{2L} . \tag{2-42}$$

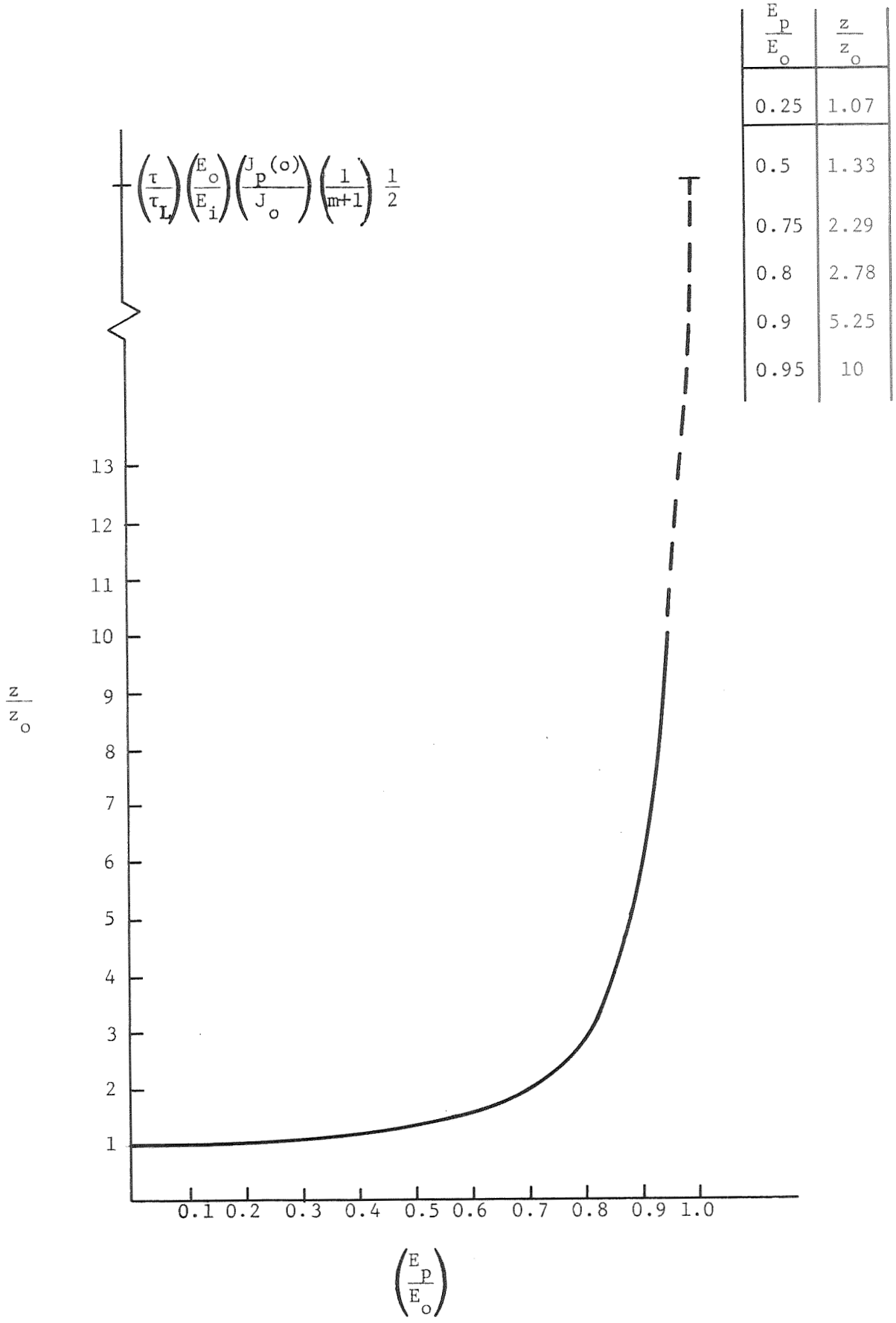

$\frac{E_p}{E_o}$	$\frac{z}{z_o}$
0.25	1.07
0.5	1.33
0.75	2.29
0.8	2.78
0.9	5.25
0.95	10

Figure 2.6. The Increase in EBIC as the Beam Energy Approaches that Required to Completely Penetrate the Oxide

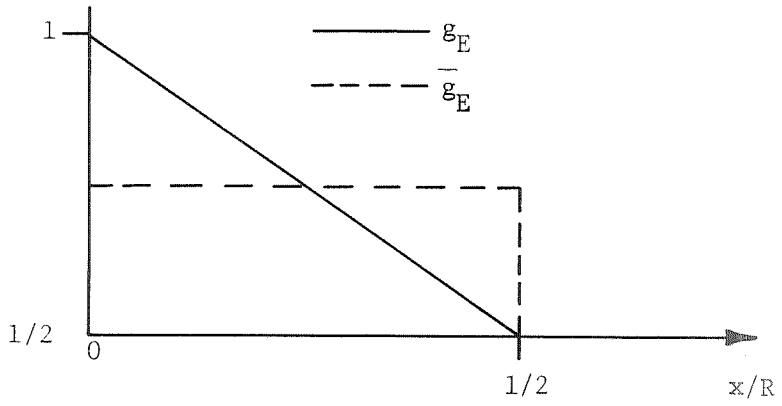

Figure 2.7. Average Generation Rate Approximation

Introducing eq. 2-42 into 2-41

$$V_a \simeq - \frac{J}{q\mu\tau_n} \int_o^L \frac{dx}{1 - \frac{x}{2L}} \tag{2-43}$$

and using the change of variable $\frac{x}{2L} = y$

$$V_a \simeq - \frac{2LJ}{q\mu\tau_n} \int_o^{1/2} \frac{1}{1-y}\, dy = \frac{2LJ}{q\mu\tau_n} \ell n \frac{1}{2} \tag{2-44}$$

or

$$J = - \frac{q\mu\tau_n V_a}{2L\ell n2} . \tag{2-45}$$

We should compare the result of

$$\frac{J}{q\mu} \int_o^L \frac{dx}{\bar{g}_E\tau_n + n_o} = - \int_o^{V_a} dV_a \tag{2-46}$$

where $\bar{g}_E\tau \gg n_o$ for $0 \leq x \leq L$.

Using $\bar{g}_E = 3/4$ (from Fig. 2.7) and

$$V_a = - \frac{J}{q\mu\tau_n 3/4} \int_o^L dx = - \frac{JL\ 4}{q\mu\tau_n 3} . \tag{2-47}$$

Thus,

$$J = - q\mu\tau_n \frac{V_a}{L}\left(\frac{3}{4}\right) . \qquad (2\text{-}48)$$

Comparing eqs. 2-45 and 2-48 indicates that our approximation should be valid to at least an order of magnitude for m = 1 for penetrating beams where essentially linear behavior is expected over an appreciable portion of the sample.

To obtain an estimate of z_{max} we need a new average generation rate for $R \geq L$ where

$$\bar{g}_E = \frac{1}{L}\int_o^L g_E(x)\, dx . \qquad (2\text{-}49)$$

Then we must consider the current density where

$$J = q\mu(\bar{g}_E\tau_n + n_o)\mathcal{E} = - q\mu(\bar{g}_E\tau_n + n_o)\frac{V_a}{L} . \qquad (2\text{-}50)$$

From eqs. 2-17 and 2-49,

$$\bar{g}_E = \frac{b\rho J_p(o)}{2qE_iE_pL}\int_o^L \left(1 - \frac{b\rho x}{E_p^2}\right)^m dx \qquad (2\text{-}51)$$

where the integration yields

$$\bar{g}_E = \frac{E_pJ_p(o)}{2qE_iL(m+1)}\left\{1 - \left[1 - \left(\frac{E_o}{E_p}\right)^2\right]^{m+1}\right\} . \qquad (2\text{-}52)$$

The ratio of the induced current density to the irradiated beam current density is

$$\frac{J}{J_p(o)} = z = - \frac{J_o}{J_p(o)} - \frac{q\mu V_aE_p\tau_n}{2qE_iL^2(m+1)}\left\{1 - \left[1 - \left(\frac{E_o}{E_p}\right)^2\right]^{m+1}\right\} \qquad (2\text{-}53)$$

where J_o is the unirradiated current density. Defining $z_o = \frac{J_o}{J_p(o)}$

and considering eq. 2-53 yields

$$\frac{z}{z_o} = 1 + \frac{1}{2}\frac{J_p(o)}{J_o}\frac{E_p}{E_i}\frac{\tau_n}{\tau_L}\frac{1}{(m+1)}\left\{1 - \left[1 - \left(\frac{E_o}{E_p}\right)^2\right]^{m+1}\right\}. \qquad (2\text{-}54)$$

We may now proceed to find z_{max} by considering

$$\frac{d\left(z/z_o\right)}{d\left(E_p/E_o\right)} .$$

Carrying out the differentiation and setting

$$\frac{d\left(z/z_o\right)}{d\left(E_p/E_o\right)} = 0 \text{ yields}$$

$$1 - \left[1 - \left(\frac{E_o}{E_p}\right)^2\right]^{m+1} - 2(m+1)\left(\frac{E_o}{E_p}\right)^2\left[1 - \left(\frac{E_o}{E_p}\right)^2\right]^m = 0 . \qquad (2\text{-}55)$$

It is obvious that we must consider specific values of m before a solution can be obtained. The value of m is usually near unity and we will obtain solutions for m = 1, 2 to obtain the general behavior. To facilitate the calculation, let $\left(\frac{E_o}{E_p}\right)^2 = x$; then we must consider

$$1 - (1-x)^{m+1} - 2(m+1)x\,(1-x)^m = 0 \qquad (2\text{-}56)$$

where for m = 1

$$3x^2 - 2x = 0$$

or

x = 0, 2/3 are the roots of eq. 2-56. Thus $(z/z_o)_{max}$ occurs for $E_p = \sqrt{3/2}\ E_o = 1.225\ E_o$ and m = 1. For m = 2 the analysis proceeds in a similar manner and a value $E_p \cong 1.6\ E_o$ is obtained for $(z/z_o)_{max}$.

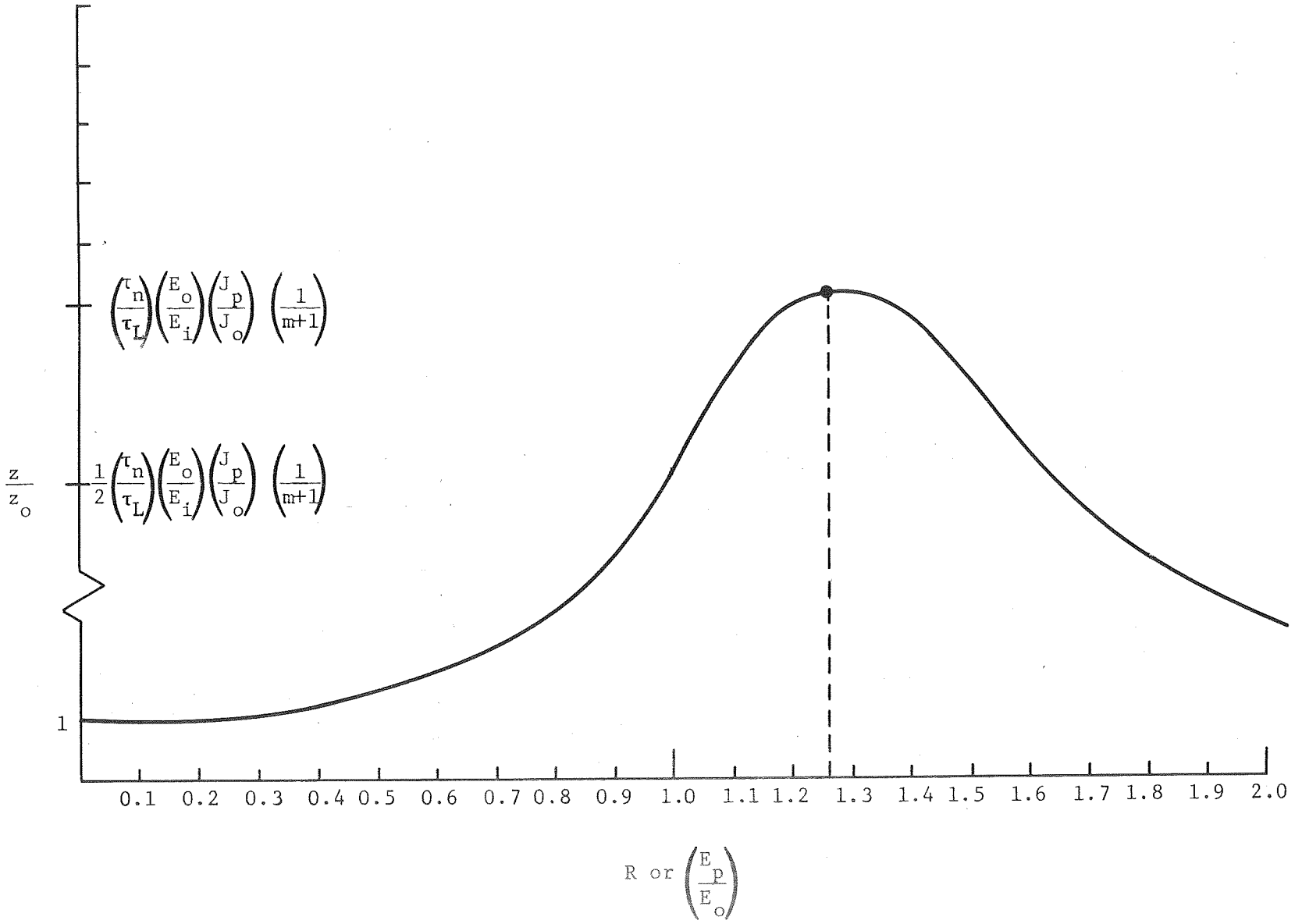

Figure 2.8. EBIC as a Function of Incident Beam Energy

Considering the m = 1 case the value of z/z_o at $E_p = 1.225\ E_o$ is, from eq. 2-41,

$$\left(\frac{z}{z_o}\right)_{max} \cong \frac{J_p(o)}{J_o}\,\frac{E_o}{E_i}\,\frac{\tau_n}{\tau_L}\,\frac{1}{m+1} \qquad (2\text{-}57)$$

where the factor $\frac{1}{m+1}$ is not evaluated so that a meaningful comparison with eq. 2-39 can be obtained. Thus, for m = 1 the maximum value of z/z_o is about twice that for $E_p = E_o$. This result is shown in Fig. 2.8 where the peak is $E_p = 1.225\ E_o$ for m = 1.

To proceed with a worst case analysis we will consider values to be used in eq. 2-57. We should recognize that $z_o = \frac{J_o}{J_p(o)}$ and the electron bombardment induced current is

$$J = J_p(o)\,\frac{E_o}{E_i}\,\frac{\tau_n}{\tau_L}\,\frac{1}{m+1}\ . \qquad (2\text{-}58)$$

We will consider m = 1, and should obtain estimates for

$$\frac{E_o}{E_i} \text{ and } \frac{\tau_n}{\tau_L}\ .$$

According to Hauser [ref. 2.6] $E_i \gtrsim 3/2\ E_g$ where E_g is the band-gap of a direct band gap semiconductor. Thus $E_i \simeq 12$ eV for SiO_2. We are interested in 1.0 μm and 0.4 μm oxides. For the sake of the discussion we will consider 1.5 μm which is an upper limit and provides a worst case analysis. The range of 10 keV electrons is approximately 1.5 μm; thus $E_o \simeq 10$ keV. Goodman reports a mobility for electrons of ~ 30 $\frac{cm^2}{V\text{-}sec}$ and a mobility lifetime product of 10^{-9} cm^2/volt. Thus, the electron lifetime is approximately $\tau_n \simeq 3 \times 10^{-11}$ seconds [ref. 2.7]. If we scale the bias for the 1.5 μm to 90 volts we may obtain an estimate for τ_L where $\tau_L = \frac{L^2}{\mu V_a} = 8 \times 10^{-12}$ seconds. Therefore,

$$J = J_p(o)\left(\frac{10^4}{12}\right)\frac{3 \times 10^{-11}}{8 \times 10^{-12}} \cong 3 \times 10^3\ J_p(o)\ . \qquad (2\text{-}59)$$

The maximum effect due to EBIC would occur if all the electrons which strike the SiO_2 capacitor structure had an energy of approximately 10 keV.

Thus, we will consider the electron flux with energy greater than 0 given as $2.55 \times 10^{11} \frac{\text{electrons}}{\text{cm}^2 - \text{day}}$ in the NASA memo dated August 19, 1970 [ref. 2.8].

Thus, one beam current density is $J_p(o) \simeq 5 \times 10^{-13} \frac{\text{amps}}{\text{cm}^2}$ and assuming a monoenergetic beam of energy 10 keV yields a worst case EBIC current density of $J \simeq 1.5 \times 10^{-9}$ amp/cm^2 for the SiO_2 capacitor structure.

For worst case the EBIC component is predicted to be 3×10^{-8} Amps (assumes a capacitor area of 20 cm^2). This value is small or comparable to the dark current leakage. Consequently EBIC is not expected to be a significant factor during the MTS flight.

SECTION II. REFERENCES

2.1 Whiddington, R: Proc. Roy. Soc. (London) A86, 360 (1911); A89, SS4 (1913).

2.2 Williams, E. J.: Proc. Roy. Soc. (London) A130, 310 (1931).

2.3 Evans, R. D.: The Atomic Nucleus, McGraw-Hill Book Company, p 623, (1955).

2.4 Lenard, P.: Ann. Physik 12, 714 (1903).

2.5 Pensak, L.: Phys. Rev. 75, 472 (1966).

2.6 Hauser, J. R.: J. Appl. Phys. 37, 507 (1966).

2.7 Goodman, A. M.: Phys. Rev. 152, 785 (1966); Phys. Rev. 152, 780 (1966).

2.8 Memo to Dr. J. R. Davidson from Charles V. Woerner, "Computer Maps for Electron-Proton Environment," dated August 10, 1970.

SECTION III

CHARGE SEPARATION EFFECTS

One of the most pronounced effects of ionizing radiation on the MOS system is the introduction of a semipermanent, positive space charge into the oxide layer. This radiation-induced space charge buildup has been characterized extensively for oxides exposed to various types of ionizing radiation [refs. 3.1-3.6], and it is believed that the charge buildup can be described by the following process:

> Electron-hole pairs are generated within the silicon dioxide by the ionizing radiation. The electrons, having a higher mobility-lifetime product than the holes, escape the oxide in greater numbers than do the holes, leaving a net positive charge trapped within the oxide. This process continues until the hold traps are saturated or until equilibrium is reached between the rates of charge buildup and decay.

The trapped oxide charge is generally assumed to lie within a few hundred angstroms of the silicon-oxide interface when the gate bias applied during irradiation is positive. The magnitude of this oxide charge is strongly dependent on gate bias during irradiation and increases almost linearly with bias up to trap saturation [refs. 3.3-3.5]. The fact that the image charge reflected at the silicon surface is greater for positive than for negative gate biases suggests oxide charge accumulation near the metal electrode for the negative bias irradiations.

The oxide space charge is "semipermanent" at room temperature but can be annealed optically or at elevated temperatures. Annealing studies have shown the annealing rate to be a very strong function of temperature [refs. 3.6, 3.7]. Room-temperature annealing has been observed at RTI in thermal oxides irradiated with both low energy electrons [ref. 3.6] and with pulsed 600 keV electrons. However, since annealing rates vary considerably among thermal oxides prepared under different conditions, a worst-case assumption would be that annealing effects can be neglected and oxide space charge continues to accumulate with increasing fluence.

Ionization effects can be expected from both the protons and electrons of the MTS radiation environment. Protons are on the order of 50 times more effective than electrons for producing ionization damage [ref. 3.8]. However, since in the MTS environment the electron flux is approximately 600 times greater than the proton flux, proton effects will be relatively small in comparison with electron damage.

The radiation sensitivity of silicon dioxide, which is strongly dependent on processing conditions, impurity content, and other factors

not all of which have been positively identified, varies considerably among oxides prepared by different manufacturers and occasionally even among oxides prepared by the same manufacturer. Thus, it is very difficult to predict exactly how much space charge will be induced in a particular oxide at a given radiation and bias level unless considerable experimental data is available on that oxide. Lacking such data, one can however make a worst-case estimate of space charge build-up by utilizing existing models for space charge formation and published data on irradiated oxides. Extreme worst-case estimates for charge build up as a function of electron fluence in both the 0.4 μm and 1.0 μm MTS capacitors have been made and are plotted in Fig. 3.1. These curves are extrapolated from charge build-up data measured on dry oxygen prepared thermal oxides irradiated under +4 V bias with 20 keV electrons. The following assumptions assure that the curves of Fig. 3.1 are worst case.

1. The MTS capacitor oxides were prepared from wet oxygen. Wet oxygen or steam-grown oxides generally exhibit less charge build-up during irradiation than do even the most radiation resistant oxides grown in a dry oxygen environment.

2. Twenty keV electrons dissipate more energy and thereby produce more ionization damage in SiO_2 having a film thickness less than 1 μm than do higher energy electrons. Most of the electrons in the MTS radiation environment have energies well in excess of 20 keV.

3. The data of Fig. 3.1 were extrapolated from +4 V to 40 V and +60 V biases assuming a linear bias dependence with no provision for trap saturation. In reality the dependence of charge build-up on applied bias is less than linear--being closer perhaps to $V^{1/2}$. This is particularly true at high bias levels and in steam-grown oxides as hole traps become saturated.

4. No correction has been made for charge annealing although considerable annealing can occur over long periods of low flux irradiation. The original data were taken over a relatively short time interval at a much higher flux and consequently include much less charge annealing than would be expected in the MTS environment.

Fortunately, some charge build-up data are available on an electron-irradiated, steam-grown Monsanto oxide and the measured space charge is substantially below that illustrated in Fig. 3.1. These data were also taken at RTI (Oct. 1968) during the performance of NASA Contract NAS1-8156 (though not reported in ref. 3.9). Here several MOS samples having 0.68 μm oxides were irradiated at biases up to +8V with about 4×10^{13} electrons/cm^2 accelerated through 10 keV. These data are more consistent with a $V^{1/2}$ or $V^{1/3}$ bias dependence and with the lower radiation sensitivity

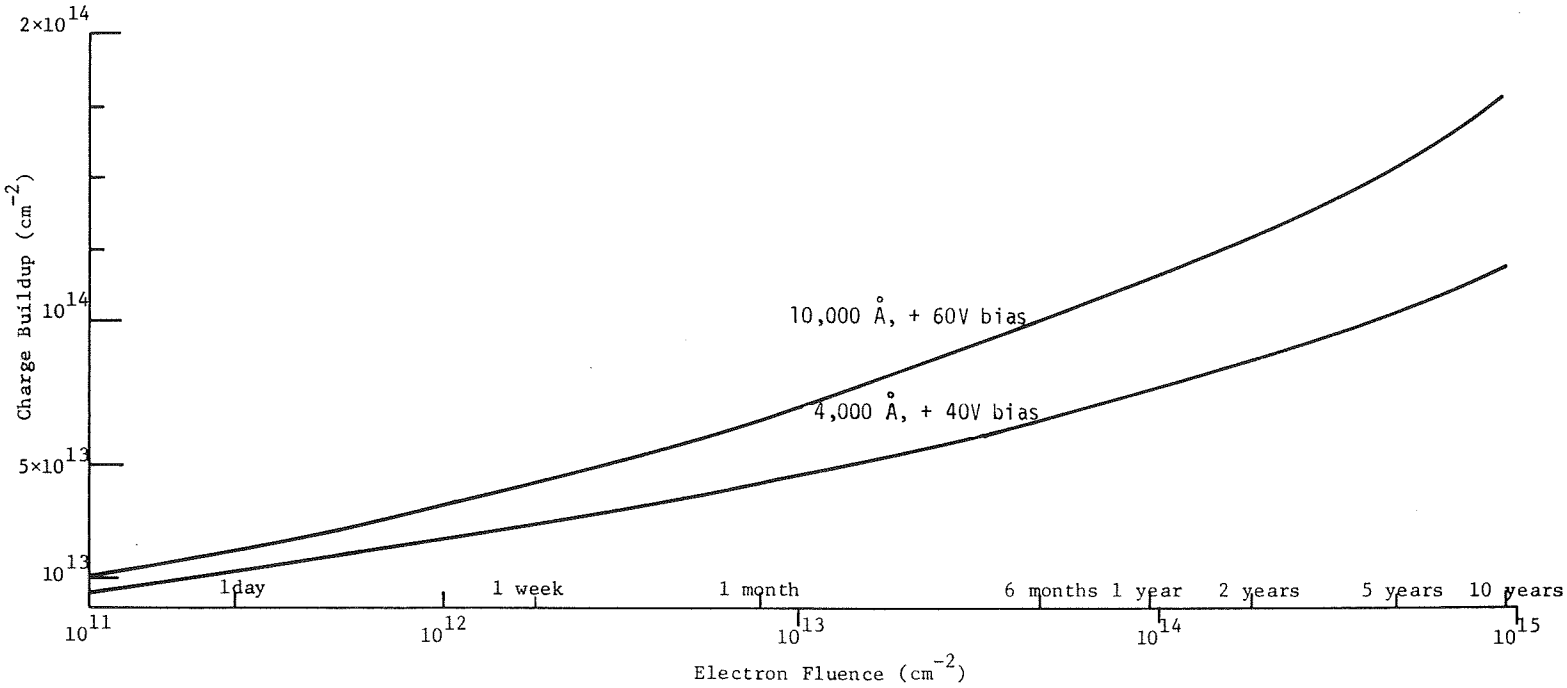

Figure 3.1. Extreme Worst-Case Oxide Charge Buildup

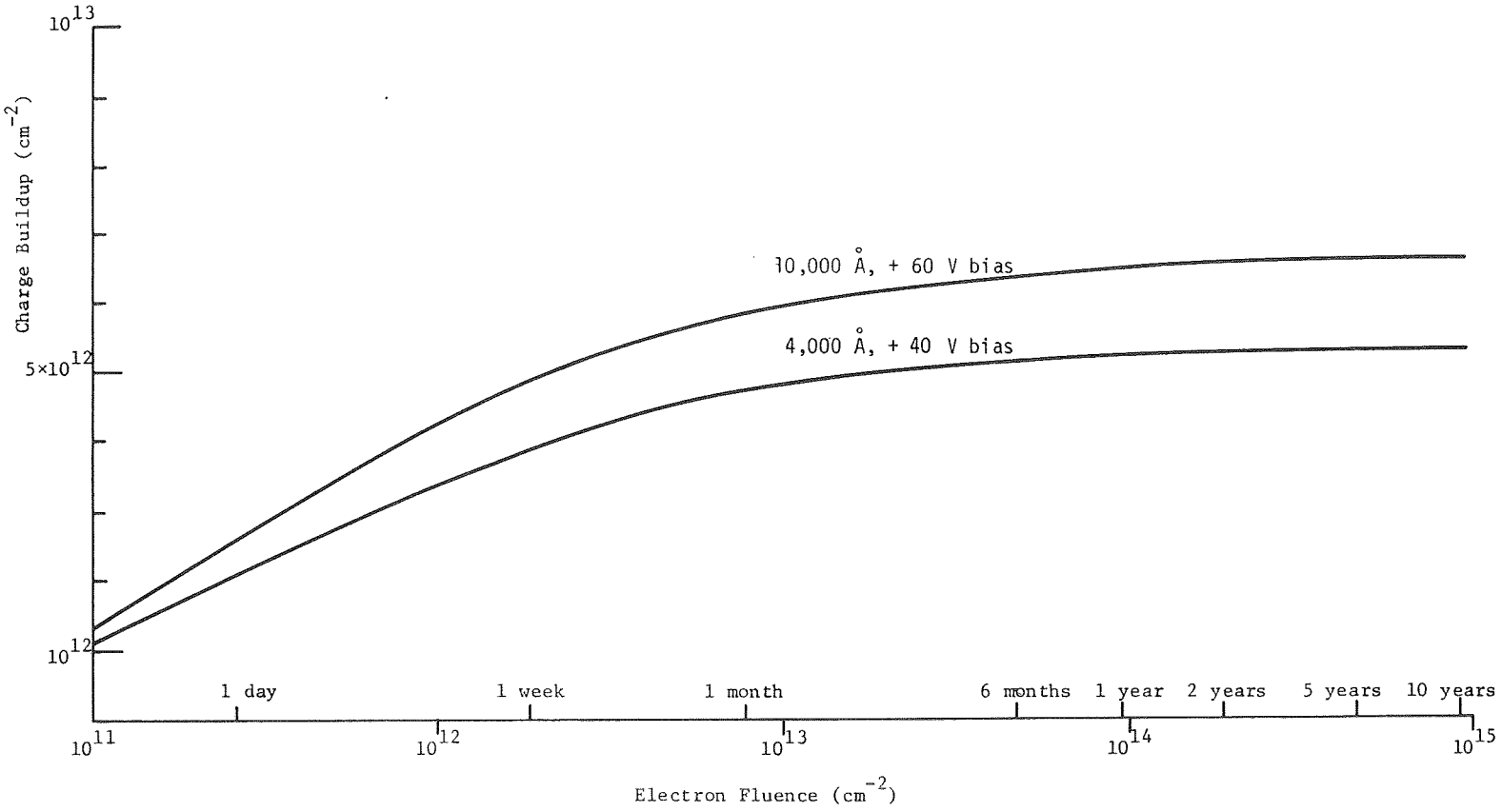

Figure 3.2. Charge Buildup in Steam-Grown Oxides Having Nominal Radiation Sensitivity

normally observed in steam grown oxides. Based on these charge build-up data and that reported in ref. 3.6 for an RTI steam-grown oxide, a second set of curves has been prepared for 0.4 μm and 1 μm oxides biased at + 40 and + 60 V, respectively (see Fig. 3.2). These curves are much more characteristic of radiation-induced positive space charge build-up in steam-grown SiO_2 and should represent a more realistic estimate of charge formation in the MTS capacitors. However, since these oxides and those of the MTS capacitors were not prepared simultaneously, there may be some difference in radiation sensitivity.

Having established estimates for the oxide space charge as a function of fluence or time in space, one is now prepared to consider the effects this space charge will have on the MTS capacitors and their operation as micrometeoroid detectors. Effects that must be considered are: 1) capacitance changes; 2) spontaneous discharge, and 3) increased leakage currents or dielectric breakdown. Sections IV and V of this report are addressed to the latter two phenomena; section III rules out the first as a problem in the MTS capacitors.

The Effect of Charge Separation Upon Detector Capacitance. - The capacitance versus voltage (C-V) characteristic is one of the more useful properties of conventional MOS structures since it allows one to measure the silicon surface potential and to characterize any space charge present in the oxide or at the oxide-silicon interface. A sharp reduction in the capacitance of an MOS structure occurs as the silicon surface layer is depleted and a depletion capacitance, C_D, is inserted in series with the larger oxide capacitance, C_{ox}. Obviously, a large and sudden capacitance change occurring in the fixed bias MTS capacitors as the oxide space charge reaches the level necessary for surface depletion would be undesirable. However, since these devices were prepared on very highly doped (.005 Ω-cm) substrates, maximum depletion region widths (~ 0.01 μm) will be quite small in comparison with oxide thickness [ref. 3.10]. Maximum capacitance variations resulting form radiation-induced changes in the silicon surface potential will be less than 1% and can be safely neglected.

REFERENCES - SECTION III

3.1 Zaininger, K. H.: Irradiation of MIS Capacitors with High Energy Electrons. IEEE Trans. Nucl. Sci., NS-13, Dec. 1966.

3.2 Grove, A. S.; and Snow, E. H.: A Model for Radiation Damage in Metal-Oxide-Semiconductor Structures. Proc. IEEE, June 1966.

3.3 Zaininger, K. H.; and Holmes-Siedle, A. G.: A Survey of Radiation tion Effects in Metal-Insulator-Semiconductor Devices. RCA Rev., Vol. 208, June 1967.

3.4 Snow, E. H.; Grove, A. S.; and Fitzgerald, D. J.: Effects of Ionizing Radiation on Oxidized Silicon Surfaces and Planar Devices. Proc. IEEE, Vol. 55, No. 7, July 1967.

3.5 Mitchell, J. P.: Radiation-Induced Space Charge Buildup in MOS Structures. IEEE Trans. on Electron Devices, ED-14, 11, November 1967.

3.6 Simons, M.; Monteith, L. K.; and Hauser, J. R.: A Study of Charge Storage in Silicon Oxide Resulting From Non-Penetrating Electron Irradiation. NASA CR-1088, June 1968.

3.7 Danchenko, V.; Desai, U. D.; and Brashears, S. S.: Characteristics of Thermal Annealing of Radiation Damage in MOSFET'S. JAP, 39, 5, April 1968.

3.8 Rosenzweig, W.: Space Radiation Effects in Silicon Devices. IEEE Trans. on Nucl. Sci., NS-12, October 1965.

3.9 Donovan, R. P.; Simons, M.; and Monteith, L. K.: The Development of Radiation Resistant Insulating Layers for Planar Silicon Technology. NASA CR-1584, May 1970.

3.10 Grove, A. S.; Deal, B. E.; Snow, E. H.; and Sah, C. T.: Investigation of Thermally Oxidized Silicon Surfaces Using Metal-Oxide-Semiconductor Structures. Solid State Electronics, Vol. 8, 1965.

SECTION IV

SPONTANEOUS DISCHARGE

Spontaneous discharge describes the possibility that the internal space charge that builds up in the oxide under irradiation can create internal electric fields in excess of the breakdown strength of the oxide, causing avalanche breakdown and discharge. Assuming blocking contacts at the insulator-metal boundary, the internal space charge cannot be neutralized by injection. Thus, we are interested in the rate of space charge build-up, the spatial distribution of the space charge and the point at which the internal field at any point exceeds the field strength of the insulator.

For SiO_2 we know that a positive charge builds up near the silicon-SiO_2 interface when the MOS device is penetrated by nuclear radiation (beta, gamma, x-ray, proton). The spatial distribution is not known. However, we will proceed with a general model to estimate the characteristics of the problem.

Consider the space charge layer shown in Fig. 4.1.

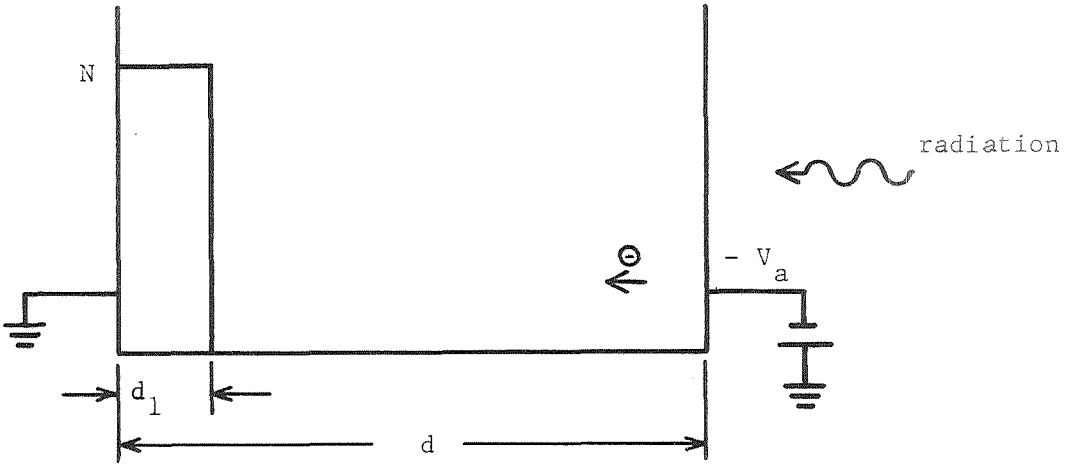

Figure 4.1. Geometry for the Analysis of Space Charge Buildup

We will consider circular symmetry. To calculate the internal electric field we assume the current density in the oxide, J, is zero. Thus,

$$\nabla^2 V = -\rho/\varepsilon \qquad 0 \le x \le d_1 \qquad (4\text{-}1)$$

$$\nabla^2 V = 0 \qquad d_1 \le x \le d \qquad (4\text{-}2)$$

where

V is the potential at the position, x,

ρ is the oxide charge density, and

ε is the dielectric constant for the oxide.

For a one-dimensional problem,

$$V(x) = -\frac{\rho x^2}{2\varepsilon} + k_1 x + k_2 \qquad 0 \le x \le d_1 \qquad (4\text{-}3)$$

and

$$V(x) = C_1 x + C_2 \qquad d_1 \le x \le d \ . \qquad (4\text{-}4)$$

Using the boundary conditions

$$V(0) = 0,\ V(d) = -V_a \text{ and } \overline{D} = \varepsilon \overline{E} \qquad (4\text{-}5)$$

is continuous at $x = d_1$, yields

$$V(x) = -\frac{\rho x^2}{2\varepsilon} + \frac{\rho d_1}{\varepsilon}\left(1 - \frac{d_1}{2d}\right)x - \frac{V_a}{d}x \qquad 0 \le x \le d_1 \qquad (4\text{-}6)$$

$$V(x) = -\frac{V_a x}{d} - \frac{\rho d_1^2}{2\varepsilon d}x + \frac{\rho d_1^2}{2\varepsilon} \qquad d_1 \le x \le d \ . \qquad (4\text{-}7)$$

The electric field is of primary interest and is given by

$$E(x) = \frac{\rho x}{\varepsilon} - \frac{\rho d_1}{\varepsilon}\left(1 - \frac{d_1}{2d}\right) + \frac{V_a}{d} \qquad 0 \le x \le d_1 \qquad (4\text{-}8)$$

$$E(x) = \frac{V_a}{d} + \frac{\rho d_1^2}{2\varepsilon d} \ . \qquad d_1 \le x \le d \qquad (4\text{-}9)$$

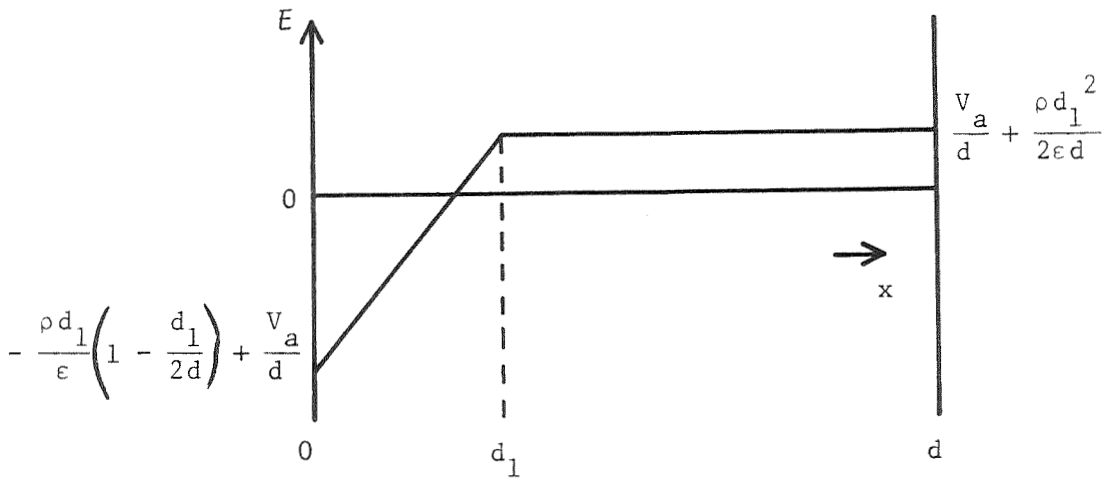

Figure 4.2. Net Internal Electric Field Under An Applied Voltage, V_a, and a Layer of Space Charge Density, ρ, Localized Between 0 and d_1

The shape of the internal field is shown in Fig. 4.2.

For our problem we should consider

$$\rho = \frac{qN}{Ad_1} \tag{4-10}$$

where N is the total number of charges in the region $0 \leq x \leq d_1$ distributed uniformly over area A. It will be convenient to use the concept of charge per unit area N_s ($\equiv N/A$) so that

$$\rho = \frac{qN_s}{d_1} \tag{4-11}$$

Thus,

$$E(x) = \frac{qN_s}{d_1\varepsilon}\left[x - \frac{d_1}{d}\left(d - \frac{d_1}{2}\right)\right] + \frac{V_a}{d} \qquad 0 \leq x \leq d_1 \tag{4-12}$$

and

$$E(x) = \frac{V_a}{d} + \frac{qN_s d_1}{2\varepsilon d} \; . \qquad d_1 \leq x \leq d \tag{4-13}$$

Since we are interested in spontaneous discharge, the local electric field must exceed the breakdown field strength in that region. We will assume that for $N_s = 0$ there is no breakdown or that V_a/d is small compared to the field necessary to initiate discharge in any region. This assumption says that the clearing voltage is large with respect to the operating voltage (the clearing voltage is that voltage to which the capacitor has been subjected during manufacture in an operation designed to remove weak spots in the oxide). For the capacitors to be flown on MTS this assumption is marginal. The 0.4 μm oxide capacitors have been cleared to 85 volts and are operated at 40 volts; the 1.0 μm oxide capacitors have been cleared to 150 volts and are operated at 60 volts. Low voltage discharges, similar to those that occur during clearing, are expected to occur if the radiation induced space charge builds up an internal field exceeding that placed across the capacitor during clearing.

The maximum electric field will occur at $x = 0$ for the uniform distribution and $d_1 < d$.

$$E_{max} = E(0) = -\frac{qN_s}{\varepsilon d}\left(d - \frac{d_1}{2}\right) + \frac{V_a}{d} . \qquad (4\text{-}14)$$

Thus, for the above assumptions our primary concern is

$$E_{max} = -\frac{qN_s}{d}\left(d - \frac{d_1}{2}\right) \qquad (4\text{-}15)$$

where $\frac{V_a}{d}$ has been neglected. There are two extremes: (1) $d_1 << d$ for which

$$E_{max} = -\frac{qN_s}{\varepsilon} \qquad (4\text{-}16)$$

and (2) $d_1 = d$ for which

$$E_{max} = -\frac{qN_s}{2\varepsilon} . \qquad (4\text{-}17)$$

Assuming N_s to be the same in both situations, the maximum field differs by only 1/2 for these two extreme distributions. With only a factor of two involved, the spatial distribution is not crucial to the determination of the maximum internal field. However, we will find that it is very important in determining the characteristic of a discharge event as detected by current flow in the external circuit.

Figure 4.3 shows the dependence of the maximum electric field $|E_{max}|$

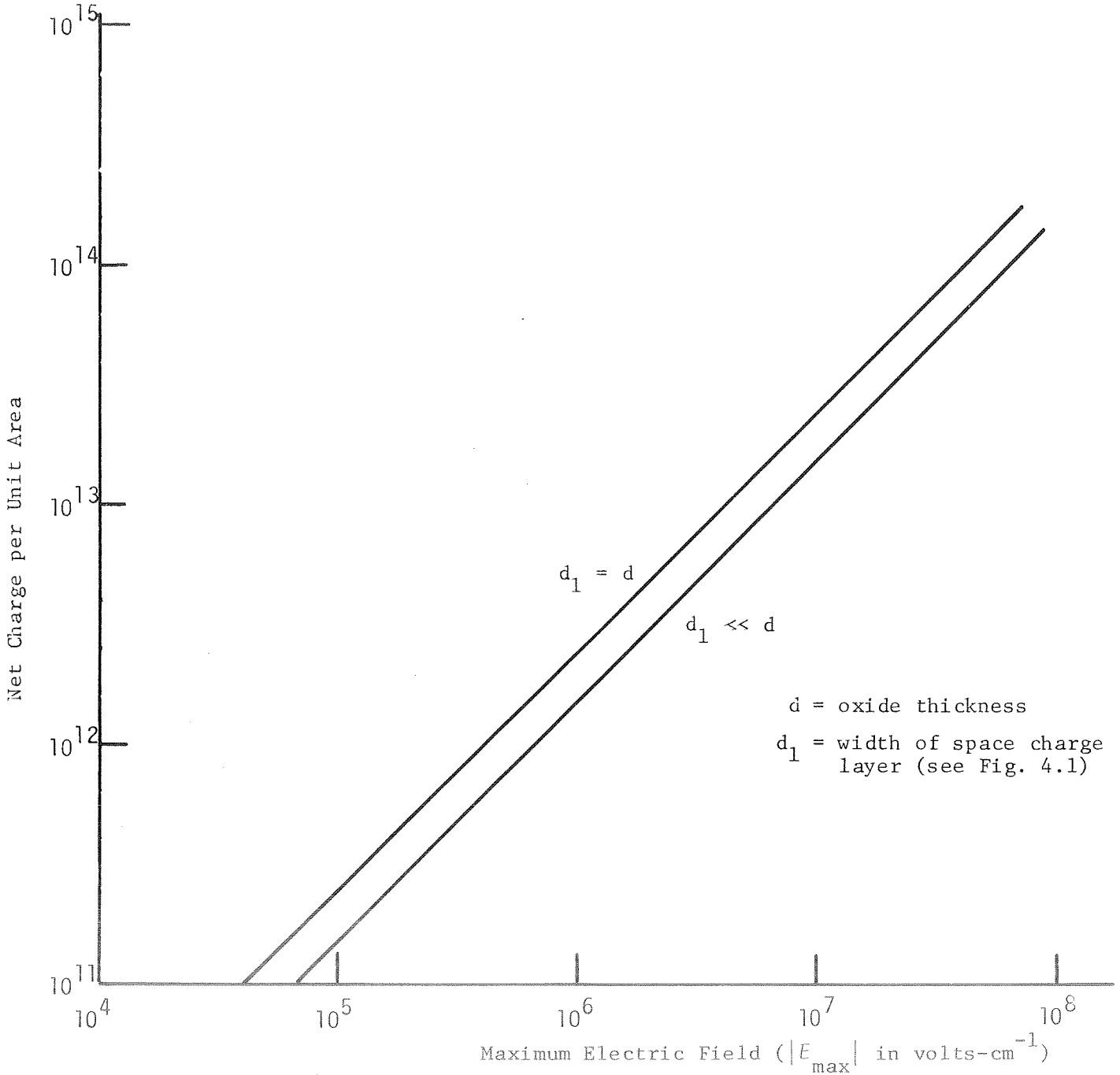

Figure 4.3 Calculated Maximum Electric Field in the Oxide as a Function of Space Charge Buildup.

upon the charge density N_s. We will find it convenient to use the results of Fig. 4.3 to estimate the performance of a SiO_2 dielectric in a nuclear radiation environment. However, to fully analyze the spontaneous discharge event, an estimate of the space charge spatial distribution will be obtained before proceeding.

We will estimate the extent of the space charge region by considering the difference in mean free path of the ionized electrons and holes. The mean free path, L, is given by

$$L = \mu E \tau = \frac{\mu V \tau}{d} \tag{4-18}$$

where

μ is the carrier mobility,

τ is the free carrier lifetime, and

E is the field in which the carrier drifts.

During early space charge buildup the electric field is $\frac{V_a}{d}$; thus we will calculate a minimum mean free path. Using values obtained by Goodman where $\mu_n \tau_n \simeq 10^{-9} cm^2/volt$ and $\mu_p \tau_p \lesssim 10^{-10} cm^2/volt$ yields

$$L_n = 10^{-9} E \text{ cm} \tag{4-19}$$

and

$$L_p = 10^{-10} E \text{ cm}. \tag{4-20}$$

Our basic assumptions concerning the radiation induced space charge are:

1) Uniform ionization of hole electron pairs throughout the SiO_2 film;
2) All ionized carriers travel their mean free path before being trapped;
3) Trapping predominates over recombination,
4) Diffusion of free carriers is negligible.

Under these assumptions the model is rather trivial; however, it represents the conditions for spreading the charge over the maximum distance. Relaxing any of the above assumptions complicates the model and tends to restrict the spatial distribution of the space charge. To remove all the assumptions would result in a completely general solution, but so far that problem has proven to be insoluble.

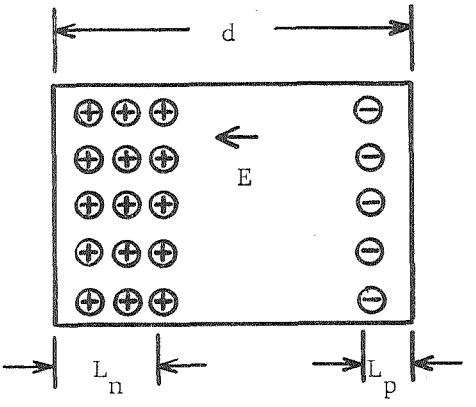

Figure 4.4. Radiation Induced Space Charge Regions

Although a complete analysis is not available, the simple model can crudely illustrate the spatial dependance upon the mean free paths of the charge carriers. Consider Fig. 4.4 where $L_n >> L_p$ and $L_n < d$ (d is the sample thickness).

There will be a positive space charge over a region, L_n, and a negative space charge over the region, L_p, near the electrode with the positive potential. In the intervening region n = p and recombination predominates. In the space charge regions there is a deficiency and trapping predominates to yield the space charge. As the applied electric field is increased, the space charge layers will grow and when $L_n = d$ the positive layer will reach a maximum and the overlapping region, L_p, will be neutralized. Thus, we may obtain a space charge over only a portion of d. When $L_n + L_p = d$, the maximum spatial extent exists. As the voltage is further increased the space charge layer is neutralized until $L_p = d$ where the internal space charge should again be neutralized throughout. Assuming d = 1.0 μm and $L_n \gtrsim 10\ L_p$, the space charge should extend from the silicon interface to 0.9d for an applied field of approximately 10 volts. For the intended operation of 60 volts bias the space charge would be neutralized to $L_p \cong 0.6$ μm or a space charge region of 0.4 μm. We will proceed with the worst case assumption of a spatial distribution throughout.

For the 0.4 μm SiO_2 layer operated at 40 volts both L_n and L_p are greater than the oxide thickness. Thus, the simple model predicts a completely neutralized space charge. Clearly a worst case analysis would be the maximum space charge density extended throughout the sample. This is more reasonable than our result of complete neutralization which conflicts with observation (see Fig. 3.2). Competition between trapping and

recombination for $L_p + L_n > d$ certainly retards neutralization. Therefore, for our present problem we will assume that the radiation induced space charge referred to the silicon interface by a MOS capacitance measurement is uniformly distributed throughout the volume of the SiO_2 layer.

To proceed with the analysis of spontaneous discharge we will consider earlier results presented by Monteith [ref. 4.1]. The transient across the load resistor in Fig. 4.5 can be analyzed by calculating the external charge transfer resulting from spontaneous discharge. The applied voltage, V_a, is neglected consistent with our previous discussion. When $|E_{max}|$ is large enough to initiate breakdown at the surface, the value of charge liberated can range from the total space charge in the sample to only an infinitesimal volume of charge in the region near an isolated defect. For a localized breakdown the amount of charge liberated is probably confined to the region near the defect since the remainder of the SiO_2 film is not subjected to either the localized field or the reduced field strength associated with defect. Also the clearing operation to prepare the large surface SiO_2 detectors is further evidence for localized breakdown. Thus, it is expected that defect breakdown may be approximated by assuming a variable field strength and a variable volume of liberated charge in the spontaneous discharge event. To do this consider Fig. 4.6 where only a portion of the sensor is irradiated and breakdown occurs in a volume less than or equal to the irradiated volume.

Ref. 4.1. L. K. Monteith, "Study of Electron Irradiation Effects on Capacitor-Type Micrometeoroid Detectors," Final Report NAS1-3892, June 1965.

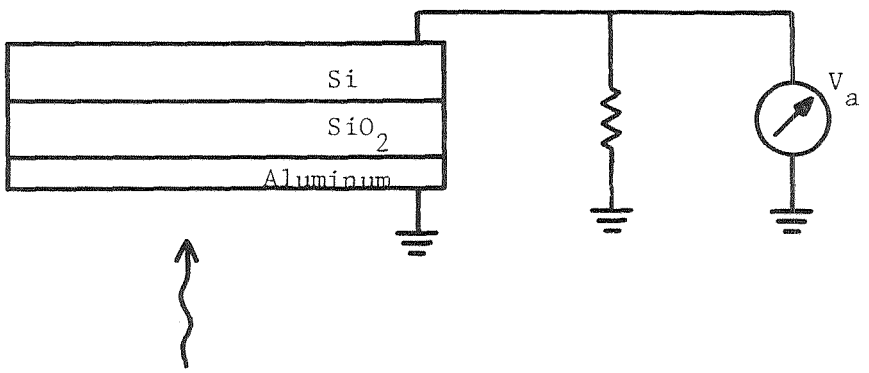

Figure 4.5. Circuit for the Analysis of External Charge Transfer During Spontaneous Discharge

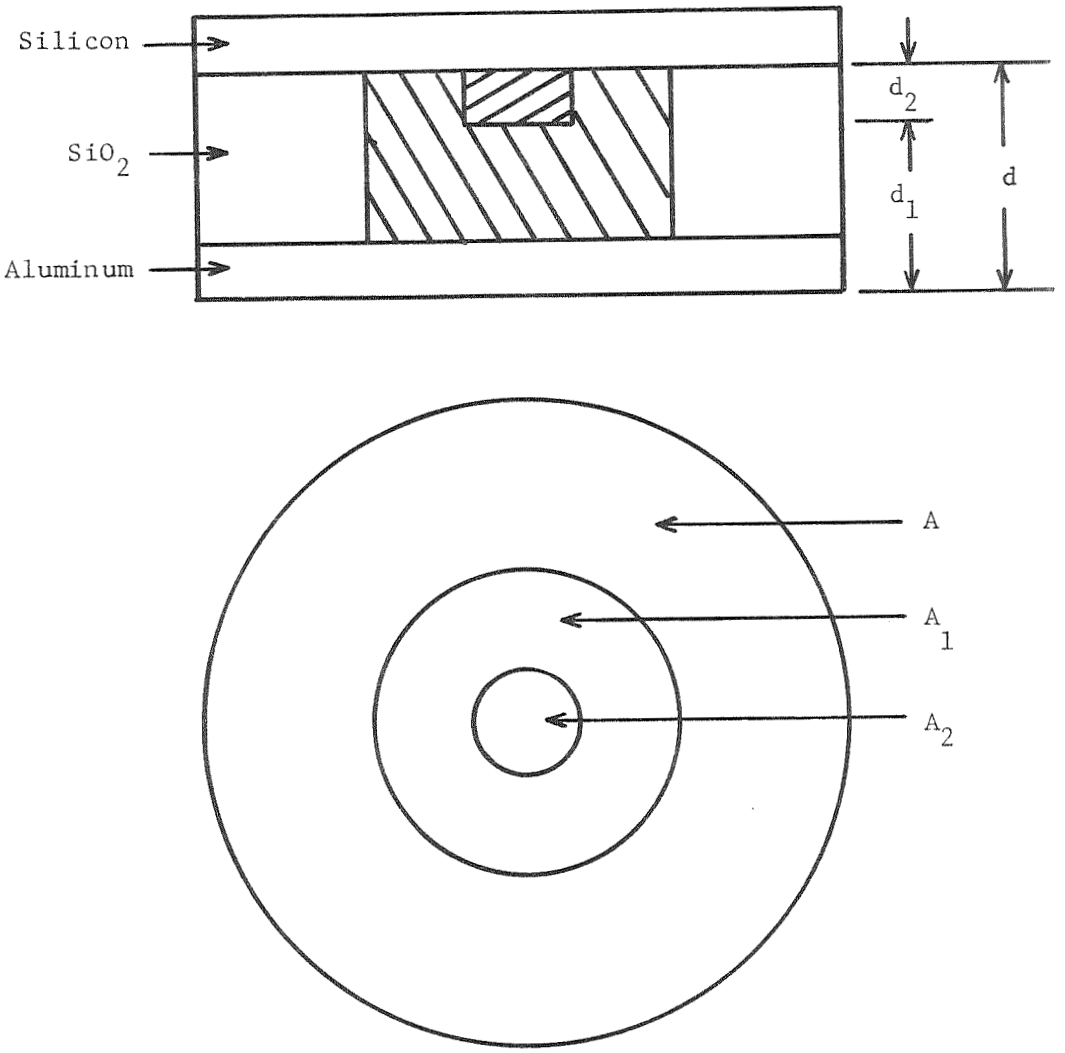

d = thickness of SiO_2

d_2 = depth of discharge

A = area of MOS capacitor

A_1 = area of irradiation

A_2 = area of discharge

Figure 4.6. Geometry for Calculating the Magnitude of Sponteneous Discharge

Assuming that the maximum extension of the discharge region parallel to the electrodes is greater than the thickness of the SiO_2 ($d_2 > d$) permits one to consider the various regions of the structure independently.

If breakdown occurs to the silicon and removes a volume $A_2 d_2$ of

space charge, the surface charge density over area A_2 on the aluminum electrode can be obtained before and after the spontaneous discharge event. If the liberated charge is assumed to recombine in the silicon in zero time, the difference between the values of surface charge density over area A_2 on the aluminum before and after the discharge event represents the charge which must be transferred from the aluminum to the silicon through load resistor, R_L, to reach an equilibrium state of charge distribution. Since D_x is continuous across the boundary at $x = 0$, the magnitude of the surface charge density over A_2 before breakdown (σ_B) on the aluminum is

$$\sigma_B = |D_x(o)|_B = \varepsilon |E_{max}|_B = \frac{qN_s}{2} . \tag{4-21}$$

For the stated assumptions the magnitude of the surface charge density over A_2 after breakdown (σ_A) on the aluminum is

$$\sigma_A = D_x(o)_A = \varepsilon |E_{max}|_A = \frac{qN_{SA}}{d}\left(d - \frac{d_1}{2}\right) , \tag{4-22}$$

where N_{SA} is the space charge per unit area after the discharge. We should realize that $N_S \neq N_{SA}$; however, the number density is the same or $\frac{N_S}{d} = \frac{N_{SA}}{d_1} = N_t$ where N_t is the number density. Therefore, the net surface charge which must be transferred from the aluminum to the silicon as a result of the breakdown is

$$\begin{aligned} \sigma_s = \sigma_B - \sigma_A &= \frac{qN_t d}{2} - \frac{qN_t d_1}{d}\left(d - \frac{d_1}{2}\right) \\ &= \frac{qN_t d_2^{\,2}}{2d} . \end{aligned} \tag{4-23}$$

The MOS device is a capacitor and the voltage developed by the discharge events is given by

$$V = V_C\, e^{-t/R_L C} \tag{4-24}$$

where C is the capacitance of the MOS capacitor detectors and the voltage appears across a load resistor, R_L, in the external circuit. The value

of V_C is determined by t = 0+ conditions across the capacitor associated with the discharge or

$$\sigma_S = \frac{Q}{A_2} = \frac{C}{A_2} \; V_C \quad . \tag{4-25}$$

Thus, V_C, is given by

$$V_C = \frac{qN_t d_2^{\,2} A_2}{2Cd} = \frac{qN_S A_2}{2C}\left(\frac{d_2}{d}\right)^2 . \tag{4-26}$$

If we introduce the concept of capacitance per unit area, $C_A = \frac{C}{A}$ yields

$$V_C = \frac{qN_S}{2C_A}\frac{d_2}{d}\frac{V_2}{V_C} \tag{4-27}$$

where V_2 is the volume associated with the discharge event and V_C is the capacitor volume. As d_2 or V_2 decreases, the voltage developed by the discharge decreases. The maximum value for V_C is given by

$$V_{C(max)} = \frac{qN_S}{2C_A} \tag{4-28}$$

where for the 0.4 μm SiO_2 device $C_A = 7.7 \times 10^{-9}$ farads/cm^2 and for the 1.0 μm device $C_A = 3.1 \times 10^{-9}$ farads/cm^2. Considering the latter yields

$$V_{C(max)} = 2.6 \times 10^{-11} N_S \text{ volts.} \tag{4-29}$$

Referring to Fig. 4.3, a field of 10^6 volts/cm is produced by a space charge of 4×10^{12}cm^{-2}. If all the space charge is liberated in a discharge event under the stated assumptions, the voltage across the capacitor at t = 0+ would be approximately 100 volts. Correspondingly, if a field of 10^7 volts/cm is required to initiate breakdown and all the space charge is liberated, the voltage at t - 0+ would be 1000 volts. However, with isolated or defect induced breakdown the volume of charge liberated is likely to be a small fraction of the internal space charge and the voltage developed as a result of the breakdown will be much smaller than the above estimates.

Extending this simple model, we can obtain other attributes of a radiation induced breakdown event. We may easily extend the assumption of instantaneous charge release and consider a finite time for the release and recombination process. With a finite time for the discharge event the amplitude of the voltage developed across the capacitor will depend upon the load resistance in the external circuit, the capacitance of the detector and the rate of charge release induced by breakdown. To illustrate the dependence of the breakdown pulse on these parameters consider the use where the net surface charge increases linearly with time until all the liberated charge has reached the electrode where the breakdown was initiated. Thus,

$$\frac{\Delta\sigma_S}{\Delta t} = \tau \qquad 0 \leq t \leq T \tag{4-30}$$

where

τ is the net surface charge per unit time and,

T represents the finite time for charge liberation.

The resulting voltage across the capacitor due to the net surface charge is

$$\frac{\Delta V_C}{\Delta t} = \frac{1}{C_A}\frac{\Delta\sigma_S}{\Delta t} = \frac{\tau}{C_A} \quad , \quad 0 \leq t \leq T \, . \tag{4-31}$$

The voltage across the loss resistor is then given by

$$V_{R_L}(t) = \tau R_L A \left(1 - e^{-t/R_L C}\right) \qquad 0 \leq t \leq T \, .$$

The maximum value of V_{R_L} occurs for t = T or when all the liberated trapped charge has arrived at the electrode to which the breakdown occurred. For the time interval $T \leq t \leq \infty$ the normal RC circuit analysis introduced earlier applies with V_C replaced by $V_{R_L}(T)$. From the above analysis it is clear that the discharge event for a finite τ behaves as a current source of τA and a capacitor charged to $\tau A R_L$ volts at t = 0 in series with opposing currents through R_L. Clearly for $T >> R_L C$ the discharge event behaves as a current source and the capacitive effect does not provide a limitation on the maximum induced voltage. To proceed further with this analysis requires a physical description of the rate of release, τ. Although a phenomenological discription may be given, a meaningful estimate is not available. However, the salient features of the discharge event are obvious from the above discussion.

SECTION V

LEAKAGE CURRENT BUILDUP

The final failure mode to be considered under this study is failure through enhanced injection processes at the silicon-oxide interface. The current limiting process in an MOS structure biased with the metal electrode positive with respect to the silicon (as is true for the MOS Micrometeoroid Detector Capacitors) is Fowler-Nordheim tunneling at the oxide-silicon interface. The degradation mechanism considered in this section is modification of the electrode injection properties so that the leakage current across the capacitor increases with time of exposure to irradiation. Eventually this process leads to degraded performance and inability of the detector to perform its micrometeoroid counting mission. In the present configuration each capacitor is in series with a 1 MΩ resistor. Initially the effective resistance of the capacitor is much greater than that of the series resistance so essentially the full bias voltage appears across the capacitor. If, however, the leakage current through the capacitor increases with irradiation, the effective resistance of the capacitor is reduced. This process can continue until the voltage across the capacitor is actually less than that across the resistor. When the voltage drop across the capacitor is less than the value of the discharge voltage required to trigger the counting circuit (~ 6 volts in the present design), the capacitor can no longer perform its intended function.

Change of leakage current with irradiation implies a change in the injection properties at the oxide-silicon interface. Although in the previous chapter the contacts to the oxide (both the silicon and the metal contact) have been assumed to be blocking, this assumption in reality is a worst-case assumption. Ample evidence exists (such as the flow of photocurrent or the annealing of space charge buildup by subsequent irradiation at a different bias) to prove that charge flows across the oxide-silicon interface during and after irradiation. In addition the properties of the current flow reasonably fit the predictions of the Fowler-Nordheim model, showing that the current limitation originates at the oxide-silicon interface (for silicon biased negatively with respect to the metal electrode).

The failure mechanism to be discussed in this chapter is to a certain extent mutually exclusive with that of spontaneous discharge just discussed in Section IV. Any interaction which permits more electron current to flow through the barrier at the oxide-silicon interface will tend to neutralize the space charge that forms during irradiation. This neutralization minimizes the possibility of counting error due to rapid charge release in a spontaneous discharge event and adds instead a relatively low, continuous component to the leakage current which has little chance of introducing an error into the counting action. For

greatest device longevity the preferred interaction of the MOS Capacitor Detector with irradiation is a slight increase in leakage current, thereby minimizing the charge buildup discussed in previous sections. This property is possessed by many other insulators as well as evaporated or chemically deposited oxide layers. Published reports of charge accumulation in such layers show far less space charge buildup for a given exposure to ionizing radiation than does thermally grown silicon oxide. Unfortunately one cannot have both a radiation hard interface and a stable device for many contemporary applications; that is, if one enhances electron injection at the insulator-silicon interface so that space charge buildup is reduced under irradiation, he also introduces an undesired instability into device operation. A nonblocking interface injects current whether there is a space charge to be neutralized or not. In the absence of a space charge the injected carriers then either become trapped and form a space charge of their own or constitute an additional loop of current flow. For the micrometeoroid capacitor detector considered here, a positive space charge is expected to exist adjacent to the oxide-silicon interface and enhanced electron injection from the negatively biased silicon would be beneficial--at least initially. If the injection degradation proceeds beyond the levels required to maintain charge neutralization, it then dominates the device degradation under irradiation.

No information appears in the literature describing the change of current flow through an MOS capacitor as a function of electron irradiation. Previous RTI work has shown that one consequence of ion implantation of MOS capacitors is to decrease the effective resistivity of the insulator. This interaction accompanies radiation hardening of the oxide and is consistent with a reduced barrier to Fowler-Nordheim tunneling as a result of the ion implantation. That similar effects should occur with high energy electrons is not unreasonable (but, so far as can be determined, has not been demonstrated). In this previous RTI work the magnitude of the degradation observed under substantial doses of ion bombardment was not destructive of the capacitor structures. In fact, the ion implanted oxide is a better insulator for building an MOS capacitor detector so far as spontaneous discharge is concerned. The penalty is an increase in the leakage current of each capacitor by one to two orders of magnitude. This increase in leakage current is tolerable, since it should not affect the operation of the detectors. A reasonable criterion for determining when detector operation is being jeopardized by increased leakage current is a value of effective capacitor resistance equal to 10 MΩ. This value is ten times the series resistance in the present detector package and guarantees that virtually all of the applied voltage appears across the capacitor rather than the series resistor. At a bias of 40 V the present detectors exhibit leakage currents of 10^{-7} to 10^{-8} amps. Increasing this leakage current by an order of magnitude keeps the effective resistance of the capacitors above the 10 MΩ limit. Two orders of magnitude increase in leakage current (possibly as high as 10^{-5} A at 40 V) would begin to be noticeable in the detector operation and power requirements.

Leakage Current in the MTS Capacitor. - The oxidized capacitor to be used on the MTS consists of a thermally-grown silicon oxide dielectric. Previous experience with these oxides shows them to be a material of high perfection and electric breakdown strength except for pinholes or weak spots scattered throughout their bulk. These imperfections dominate the leakage current of the capacitor until they are eliminated. Many of the capacitors with 0.4 μm oxide or less exhibit nearly ohmic, low resistance characteristics between the metal and silicon electrodes immediately after fabrication. These capacitors, seemingly useless, can be salvaged by a clearing operation which consists of blowing the region of low resistance off the capacitor in a self-healing discharge event quite similar to the micrometeoroid impact itself. The procedure is to slowly increase the dc voltage across the capacitor, presumably creating very high current density through the imperfection [ref. 5.1]. Eventually the increasing current causes such a high temperature at the defect that thermal runaway occurs and the rest of the capacitor discharges through this narrow region in a dramatic, explosive, light emitting discharge. The material in the path of the discharge is vaporized so that the net effect is to neatly remove this weak spot from the capacitor. This procedure can be carried out to higher and higher clearing voltages until all weak spots are removed and the bulk properties of the uniform oxide are reached. Attempts to increase the clearing voltage above this value are unsuccessful, and, if pursued, lead to degradation and destruction.

In the production of the capacitors to be used on MTS, the clearing operation has been carried out to a voltage between 2 and 3 times the intended operating voltage of the detector. For both the 0.4 μm and the 1.0 μm detectors this value of clearing voltage is well below that necessary to reach intrinsic bulk oxide behavior. Therefore, the leakage current of the oxides to be flown on the MTS as capacitor detectors are dominated still by the properties of imperfections or weak spots scattered throughout the bulk of the oxide. To predict how leakage current, when dominated by weak spots, will deteoriate with irradiation requires knowledge of the conduction mechanisms characterizing the weak spot. No adequate model of this conduction process exists at present. The magnitude of the deterioration can be easily determined experimentally, however, as outlined in Section VI.

The properties of a defect free oxide are better understood in that an adequate model exists to explain the observed current-voltage properties. This model is described briefly in the next section.

Fowler-Nordheim Model. - The conduction properties of thin dielectric films have been studied intensively over the past ten or fifteen years and considerable data have been gathered on various combinations of metal-insulator-metal or semiconductor sandwiches. Only recently, however, has sufficient understanding and experimental finesse been available to allow models to reasonably predict the observed behavior.

Current flow through the insulator of a metal-insulator-semiconductor (MIS) sandwich can be either bulk limited or electrode limited. In the former case the current flow observed between the two metal electrodes is determined by the bulk properties of the insulator between them; in the latter case, the interfacial barrier limits the current flow. While these limiting processes are different in origin, the electrical properties of the differently limited systems do not differ greatly so that distinguishing the bulk limited case from the barrier limited case is by no means straightforward and simple.

The MOS system, consisting of metal-oxide-silicon, is an electrode limited system. This statement implies that the dc leakage current measured on any given MOS structure depends not on the bulk properties of the oxide but upon the interface between either the metal and the oxide or the oxide and the silicon, depending on the bias direction. The case to be considered here is that in which the metal is biased positively with respect to the silicon so that current flow is determined by electron ejection from the silicon into the conduction band of the oxide as pictured in Fig. 5.1. Current flow is through the thin oxide barrier separating the silicon from the conduction band of the oxide.

Tunneling through an interfacial barrier of this type is called Fowler-Nordheim tunneling, named after the investigators who first described the model. An expression describing the current flow is [ref. 5.3]:

$$J = (q^3E^2/8\pi h\phi_B)\ \exp\ [-\ 4(2m)^{\frac{1}{2}}\ (m^*/m)^{\frac{1}{2}}\phi_B^{3/2}/3hqE]$$

$$= \frac{1.54 \times 10^{-6}E^2}{\phi_B}\ \exp\ [-6.83 \quad 10^7\phi_B^{3/2}\left(\frac{m^*}{m}\right)^{\frac{1}{2}}E^{-1}] \qquad (5\text{-}1)$$

where

J is the current density (A/cm^2),

E is the applied field (V/cm),

$\frac{m^*}{m}$ is the average effective mass ratio of electrons tunneling through the oxide forbidden band to the free electron mass, and

ϕ_B is the barrier height at oxide-silicon interface (eV).

This equation fits the experimental data reasonably well for an effective mass ratio between 0.4 and 0.5. When the metal electrode is biased positively with respect to the silicon, this model predicts that the current flow is independent of the type of metal used to make contact since, under this direction of bias, the ejection is from the silicon into the conduction band of the oxide. A barrier height determined from photoemission experiments of electrons in thermal oxide is ϕ_B = 3.25 eV [ref. 5-2] (the doping of the silicon is also expected to

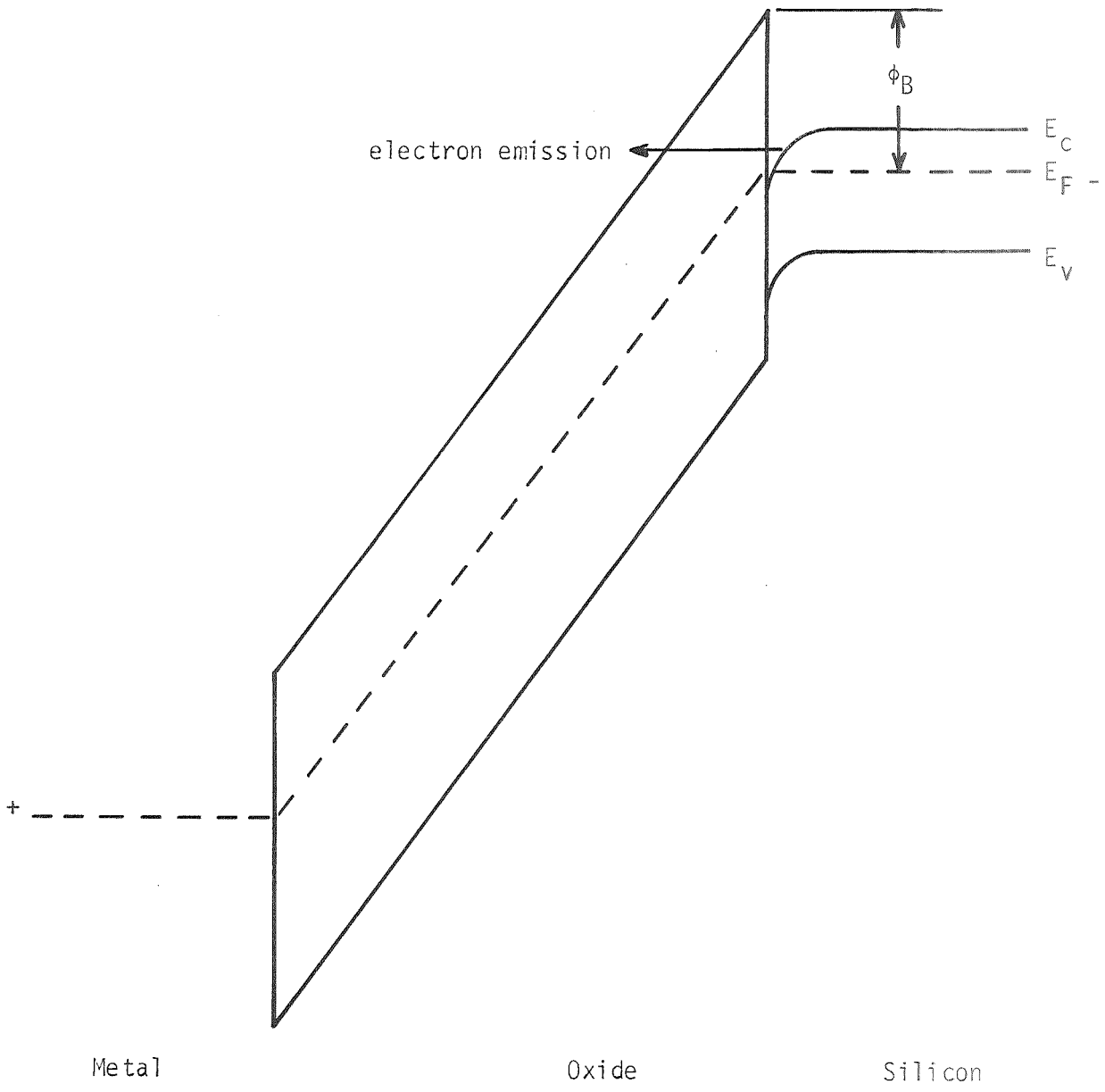

Figure 5.1. Fowler-Nordheim Tunneling at the Oxide-Silicon Interface, Metal Biased Positively with Respect to the Silicon [ref. 5.1]

be unimportant because of the severe band bending associated with such high fields (see Fig. 5.1)).

Putting $\phi_B = 3.25$ eV and $\frac{m^*}{m} = 0.42$ in eq. 5-1, yields the following relation between current density and electric field:

$$J = 4.74 \times 10^{-7} E^2 \exp\left[-2.59 \times 10^8 E^{-1}\right] \qquad (5\text{-}2)$$

Equation 5-2 holds only for MOS structures with the metal biased positively with respect to the silicon. Plots of this equation over the regions in which it can be compared with experiment are given in Fig. 5.2. The Fowler Nordheim plot [$\ln(J/E^2)$ vs $\frac{1}{E}$] is shown in Fig. 5.2a; a plot of $\ln J$ vs E appears in Fig. 5.2b. The data points can be fitted to eq. 5-2 quite well.

What is significant for the MOS Capacitor Detector, however, is that the predicted leakage currents at the planned operating field of 10^6 volts/cm or less are negligibly small (orders of magnitude less than what is actually observed). The conclusion is that the leakage current of the MOS Detector is dominated by localized defects rather than Fowler-Nordheim currents.

The clearing operation to which all these capacitors have been subjected furnishes additional evidence for the existence of defects. The clearing operation as it is now carried out (to 80 V for the 0.4 μm oxide; 150 V for the 1.0 μm oxide) eliminates the most severe defects. That other smaller defects should remain after the clearing operation to 80 or 150 volts is not an unexpected result. The measurements of leakage current that have been made suggests that the leakage current of the capacitor as a whole is determined by what flows through a large number of these localized regions of high current density.

Even if the Fowler-Nordheim model adequately described the leakage current of the MOS Detectors, the influence of irradiation upon such a structure is still an unknown. No easy solution to the problem of radiation influence in the Fowler-Nordheim model has been worked out.

Summary. - Understanding of the leakage currents flowing in the MOS Capacitor Detector is poor. For small area, defect free oxides an adequate model exists; but this model does not apply to the MOS Detector whose leakage current is defect dominated. The influence of radiation upon both the defect-free and the defect-dominated MOS structure is unknown. The magnitude of the problem can be easily determined experimentally and this solution is described and recommended in Section VI.

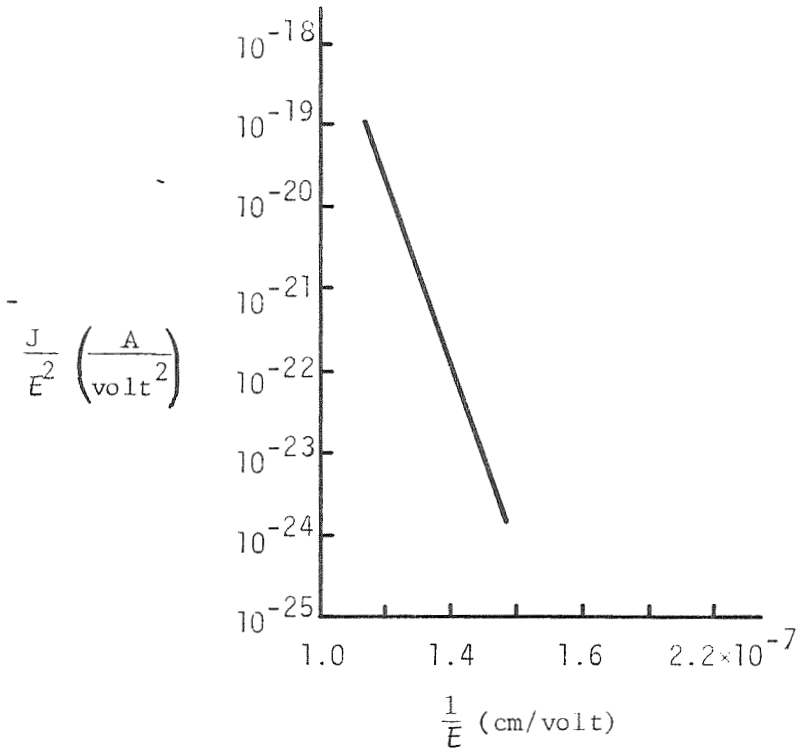

a) Fowler-Nordheim plot

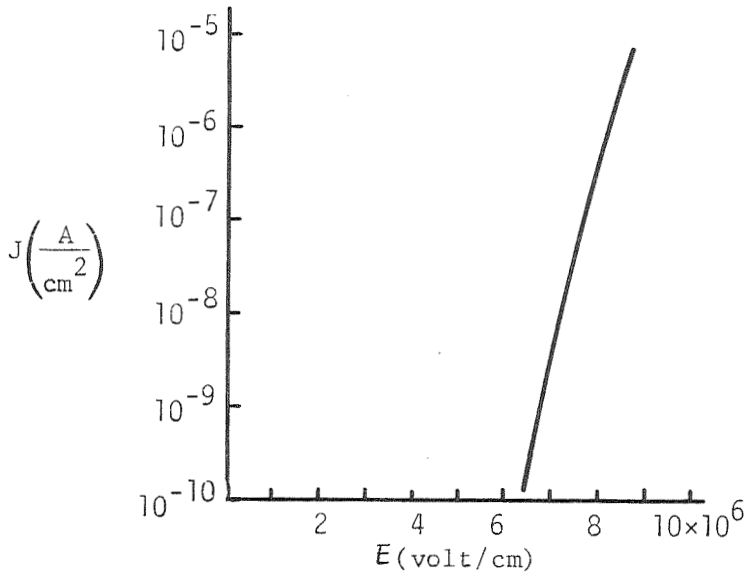

b) Semilog plot

Figure 5.2. Current Densities Predicted by Eqs. 5.1 and 5.2 for MOS Structure with the Metal Biased Positively with Respect to the Silicon [ref. 5.2]

SECTION V. REFERENCES

5.1 Klein, N.: Electrical Breakdown in Thin Dielectric Films. J. Electrochem. Soc. 116, July 1969, pp 963-972.

5.2 Lenzlinger and Snow, E. H.: Fowler-Nordheim Tunneling into Thermally Grown SiO_2. J. Appl. Phys. 40, January 1969, pp 278-283.

5.3 Snow, E. H.: Fowler-Nordheim Tunneling in SiO_2 Films. Solid State Communications 5, pp 813-815 (1967).

SECTION VI

CONCLUSIONS AND RECOMMENDATIONS

In the preceding sections the effect of charged nuclear particles upon the electrical properties of an MOS capacitor micrometeoroid detector has been considered in some detail. The primary emphasis has been upon spurious signals and catastropic failure. The spurious signals have been termed "spontaneous discharge". These signals are similar in all respects to the discharge associated with the penetration of a micrometeoroid. Therefore it is imperative that a critical assessment of the spontaneous discharge susceptibility be obtained. In addition, possible failure mechanisms should be identified so that reliability expectations can be obtained for the time interval of the mission. To provide a detailed assessment, the effects of charged particle radiation have been divided into three distinct categories: (1) radiation induced conductivity, (2) radiation induced space charge, and (3) radiation induced damage (leakage).

(1) Radiation induced conductivity could represent a problem if the conductivity was reduced such that the voltage across the detector was reduced. Since the detector is in series with a 10^6 ohm resistor, the resistance of the detector must remain in excess of 10^7 ohms if the applied voltage is to appear essentially across the detector. In Section II we have considered a 1.5 μm SiO_2 film (a worst case) with an area of 20 cm^2. With an applied voltage of 90 volts (scaling up of 60 volts on 1.0 μm oxide) and the electron flux predicted for the MTS flight a worst case analysis yields a radiation induced current of 3×10^{-8} amps. Thus, the equivalent resistance of the SiO_2 film would be 3×10^9 ohms which is well above the 10^6 ohms of the load resistor. Therefore, radiation induced conductivity associated with intrinsic ionization should not degrade the performance of the MOS capacitor micrometeoroid detector.

(2) Analysis does not provide a clear prediction of the importance of radiation induced space charge buildup and spontaneous discharge. In Section III the space charge buildup is substantially different for the worst case (Fig. 31.) and the "typical" results (Figure 3.2). Using these results in the analysis of Section IV clearly indicates the dilemma. For the worst case analysis with a surface charge density of approximately $10^{14} cm^{-2}$ throughout the MTS flight, the internal electric field due to the space charge is in

excess of 10^7 volts/cm. The maximum field for SiO_2 is 10^7 volts/cm. Thus spontaneous discharge is definitely a possibility. For the more realistic space charge buildup resulting in a surface charge of approximately 10^{12} cm^{-2}, the internal electric field is near 10^6 volts/cm. Since the detectors are cleared to a field of approximately this same value, it is difficult to predict the performance. However, one fact is imminently clear. The clearing operation removes defects or field strength weaknesses which could provide regions for spontaneous discharge with space charge buildup.

One factor which provides some encouragement is the apparent volume associated with the clearing of defects. The diameter of the regions where the clearing event occurs is less than 1 mm. Therefore, the ratio of the capacitor volume to the defect volume is greater than 5000 for a 20 cm^2 SiO_2 capacitor. Assuming the spontaneous discharge occurs in a defect region and removes the space charge throughout the defect region and that the internal field due to space charge is approximately 10^6 volts/cm, the spontaneous discharge pulse would be less than 20 millivolts. Clearly this would not present a problem for the MTS detector circuits.

(3) Paragraphs 1 and 2 discussed radiation induced effects arising from ionization and intrinsic charge transport. There is the added possibility that the electronic properties of the SiO_2 film will not remain constant with fluence. Radiation induced defects or structural changes may be evidenced in either a spontaneous signal or a catastropic failure. Presently we are unable to provide a detailed analysis; however, phenomenologically the effects are similar to our treatments in Sections II and IV. As shown in Section V the leakage current of the MOS capacitor detector is determined by the properties of defects ("weak spots") in the oxide. These are the regions that are removed by the clearing operation. Presently we do not have an adequate conceptual model for a defect dominated SiO_2 film. Current flow through weak spots can be barrier limited or bulk limited. If barrier limited, the additional radiation-induced defects introduced in the vicinity of the limiting barrier could cause barrier modifications that result in increases in leakage current; if bulk limited, the radiation-induced defects act as carrier traps which tend to inhibit charge neutralization through relaxation time processes. Consequently, charge buildup could be enhanced in the region of oxide weak spots, increasing the vulnerability of the oxide to spontaneous discharge at these defects.

Recommendations

With the numerous assumptions necessary to obtain an estimate of the effects of radiation on the MOS capacitor detector, it is advisable to conduct a series of experiments to verify the conclusions of this study. The primary areas of concern are spurious signals and excessive leakage current. Experiments to assess the seriousness of these two problems are relatively straightforward and should provide a reasonable confidence level. The major concern will be for proper instrumentation and proper scaling of the flux rate and energy for a reasonable irradiation period. Two separate experiments will be required to provide a reasonable simulation of the irradiation in space.

For the leakage current an MOS capacitor detector should be irradiated with relatively high energy electrons. Certainly a few hundred kilovolts would be sufficient to achieve the threshold for displacement damage. In fact a lower energy may be satisfactory. However, there is some uncertainty about the optimum energy and a reasonable compromise is 300 keV. The ultimate fluence of interest is $10^{15} cm^{-2}$. They key question is the flux rate. Radiation damage anneals so it is unrealistic to expose the sample to the entire fluence in a time interval that is short compared to that of radiation damage annealing. Annealing rates vary from minutes to hours. Some radiation induced defects require elevated temperature and even longer time intervals for annealing. However, we are interested primarily in the transient behavior of defects and will consider the long term effects as permanent. Therefore a reasonable compromise would be to achieve a fluence of $10^{15} cm^{-2}$ in about 10^{3} seconds or less than one hour. This could be satisfied with an irradiation beam current density of approximately 1 microamp/cm^2. If a swept beam facility is used, the instantaneous current density will be much greater than this and it may be necessary to reduce the average current density and extend the irradiation time longer still. (There is, of course, no need to extend the irradiation time if the MOS capacitor detector does not exhibit excessive leakage.)

One method for the test would be to irradiate the MOS detector under bias with a one megohm load resistor in series with the detector. Measuring the voltage across the resistor during and after irradiation would provide a realistic estimate of the leakage current problem. Assuming a bias of 40 volts across the MOS detector, a voltage drop of less than one volt across the one megohm resistor would probably be acceptable on the basis of leakage current. Assuming such a large effect is noticed, additional tests for impact discharge events would certainly be warranted. In fact, any significant change in electrical

properties should be followed by an impact experiment to make certain that the detector performance has not been changed.

The above experiment is oriented toward reliable performance of the detector. Equally important is the occurrence of spurious signals associated with spontaneous discharge. The major problems are detection of the spontaneous discharge and reasonable scaling of the flux rate to simulate a space environment. For the MTS a discrimination level of 1 volt appears adequate and should provide only a moderate challenge. The primary consideration will be enough bandwidth in the detection circuit to detect a discharge event. The rise time may be submicrosecond, requiring megahertz bandwidth to see the rise time. However, the decay time will be a fraction of a second with a 10^6 ohm load to simulate operational configuration. Therefore, the bandwidth will not be critical for preliminary observations where discharge characteristics are not of primary concern.

Scaling the flux rate will depend upon two factors. The circuit time constant should be short compared to the time required to achieve a fluence of 10^{15} cm^{-2}. Also, the relaxation time must be considered. We can only estimate this effect by noting the relaxation time for MOS devices which have been irradiated. The uncertainty in relaxation complicated matters. If the time was comparable to the MTS mission time we would ignore the problem. However, if it is short compared to the mission, anomalous effects due to scaling the flux rate may arise. As a first try a flux rate near 10^{11} cm^{-2} sec^{-1} (a beam current density of about .01 microamp cm^2) is suggested. Assuming spontaneous discharge events are noted the flux rate should be decreased. Since it is not practical to duplicate the actual flux rate of space, a study of discharge rate versus flux rate should be considered. In the event discharge events are not detected the experiment represents a worst case and provides the needed confidence for the detector performance in a nuclear environment.

Finally the question of energy for the irradiation electrons should be considered. Simons [ref. 3.6] has noted a correlation of maximum space charge buildup with energy dissipation of the primary electron in traversing the SiO_2. In fact the maximum buildup occurs when the dissipation of the primary electron is a maximum at the SiO_2-Si interface. This will occur at approximately 10-20 keV. Thus we may simulate worst case with a fluence of 10^{15} cm^{-2} electrons at 20 keV. Again if spontaneous discharge is observed, a more reasonable simulation must be considered. If discharge events are not detected, the worst case experiment again provides the necessary confidence.

The spontaneous discharge detector could be a single sweep storage oscilloscope with at least a 10 megahertz bandwidth and 100 millivolt/cm sensitivity. Biasing the MOS detector with a 10^6 ohm load resistor in series simulates the operational parameters. The input to the scope should be ac coupled across the 10^6 ohm resistor. Initially we are interested only in the occurrence of a single spontaneous discharge. A one-microamp/cm^2 beam current with 20 keV primary energy should provide a satisfactory worst case experiment. With this technique a number of MOS devices connected in parallel could be observed.